EPRI | ELECTRIC POWER RESEARCH INSTITUTE

Materials Reliability Program: Development of a Material Constitutive Model for Irradiated Austenitic Stainless Steels (MRP-135, Revision2)

2019 TECHNICAL REPORT

PORTIONS TRANSLATED

Materials Reliability Program: Development of a Material Constitutive Model for Irradiated Austenitic Stainless Steels (MRP-135, Revision 2)

3002013216

Final Report, September 2019

EPRI Project Manager
K. Amberge

All or a portion of the requirements of the EPRI Nuclear Quality Assurance Program apply to this product.

YES (NO)

ELECTRIC POWER RESEARCH INSTITUTE
3420 Hillview Avenue, Palo Alto, California 94304-1338 ▪ PO Box 10412, Palo Alto, California 94303-0813 ▪ USA
800.313.3774 ▪ 650.855.2121 ▪ askepri@epri.com ▪ www.epri.com

DISCLAIMER OF WARRANTIES AND LIMITATION OF LIABILITIES

THIS DOCUMENT WAS PREPARED BY THE ORGANIZATION(S) NAMED BELOW AS AN ACCOUNT OF WORK SPONSORED OR COSPONSORED BY THE ELECTRIC POWER RESEARCH INSTITUTE, INC. (EPRI). NEITHER EPRI, ANY MEMBER OF EPRI, ANY COSPONSOR, THE ORGANIZATION(S) BELOW, NOR ANY PERSON ACTING ON BEHALF OF ANY OF THEM:

(A) MAKES ANY WARRANTY OR REPRESENTATION WHATSOEVER, EXPRESS OR IMPLIED, (I) WITH RESPECT TO THE USE OF ANY INFORMATION, APPARATUS, METHOD, PROCESS, OR SIMILAR ITEM DISCLOSED IN THIS DOCUMENT, INCLUDING MERCHANTABILITY AND FITNESS FOR A PARTICULAR PURPOSE, OR (II) THAT SUCH USE DOES NOT INFRINGE ON OR INTERFERE WITH PRIVATELY OWNED RIGHTS, INCLUDING ANY PARTY'S INTELLECTUAL PROPERTY, OR (III) THAT THIS DOCUMENT IS SUITABLE TO ANY PARTICULAR USER'S CIRCUMSTANCE; OR

(B) ASSUMES RESPONSIBILITY FOR ANY DAMAGES OR OTHER LIABILITY WHATSOEVER (INCLUDING ANY CONSEQUENTIAL DAMAGES, EVEN IF EPRI OR ANY EPRI REPRESENTATIVE HAS BEEN ADVISED OF THE POSSIBILITY OF SUCH DAMAGES) RESULTING FROM YOUR SELECTION OR USE OF THIS DOCUMENT OR ANY INFORMATION, APPARATUS, METHOD, PROCESS, OR SIMILAR ITEM DISCLOSED IN THIS DOCUMENT.

REFERENCE HEREIN TO ANY SPECIFIC COMMERCIAL PRODUCT, PROCESS, OR SERVICE BY ITS TRADE NAME, TRADEMARK, MANUFACTURER, OR OTHERWISE, DOES NOT NECESSARILY CONSTITUTE OR IMPLY ITS ENDORSEMENT, RECOMMENDATION, OR FAVORING BY EPRI.

THE FOLLOWING ORGANIZATION, UNDER CONTRACT TO EPRI, PREPARED THIS REPORT:

Structural Integrity Associates, Inc.

THE TECHNICAL CONTENTS OF THIS PRODUCT WERE **NOT** PREPARED IN ACCORDANCE WITH THE EPRI QUALITY PROGRAM MANUAL THAT FULFILLS THE REQUIREMENTS OF 10 CFR 50, APPENDIX B. THIS PRODUCT IS **NOT** SUBJECT TO THE REQUIREMENTS OF 10 CFR PART 21.

NOTE

For further information about EPRI, call the EPRI Customer Assistance Center at 800.313.3774 or e-mail askepri@epri.com.

ACKNOWLEDGMENTS

The following organizations, under contract to the Electric Power Research Institute (EPRI), prepared this report:

Structural Integrity Associates, Inc.
9710 Scranton Road
San Diego, CA 92121

Principal Investigators
J. Rashid
N. Capps (currently EPRI)
B. Richardson
R. Dunham (retired)

This report describes research sponsored by EPRI.

EPRI acknowledges the valuable guidance provided by Steve Fyfitch, Framatome, for ensuring compatibility of the materials models in this report with the updated materials property database MRP-211, Revision 1.

This publication is a corporate document that should be cited in the literature in the following manner:

Materials Reliability Program: Development of a Material Constitutive Model for Irradiated Austenitic Stainless Steels (MRP-135, Revision 2). EPRI, Palo Alto, CA: 2019. 3002013216.

PRODUCT DESCRIPTION

Pressurized water reactor (PWR) internals components are subject to the effects of age-related degradation mechanisms, which might have to be evaluated as part of the license renewal process. To evaluate the effects of aging-related degradation mechanisms on component functionality, the integrated effects of void swelling, creep, stress relaxation, ductility degradation, and cracking—all of which are a function of component geometry, irradiation, temperature, and loading—need to be modeled and analyzed. This report describes a material behavior model for irradiated stainless steel Type 316 and Type 304 for use in performing engineering evaluation and assessment of bolted and welded connections in PWR internals components subjected to plant operating conditions. This report is an update to the Electric Power Research Institute's (EPRI's) MRP-135, Revision 1, dated March 2010.

Background

The current generation of PWR plants is approaching the end of their respective licensing periods, and multiple plants have already entered periods of extended operation. The nuclear power industry in the United States has developed inspection and evaluation guidelines for managing aging degradation in reactor vessel internals. The model described in this report is to be used in a finite-element-based analysis methodology. The model considers the effects of temperature, cold work, and irradiation on material behavior characteristics, which include elastic-plastic stress-strain curve, irradiation-enhanced creep (or simply irradiation creep), void swelling, and a material's failure limits associated with primary damage mechanisms, such as irradiation-assisted stress corrosion cracking and irradiation-induced embrittlement. Data used to revise the constitutive models in MRP-135, Revision 1, as described in the present revision of MRP-135, are contained in the newly revised MRP-211 report.

Objectives

- To make available materials properties that are applicable to the service conditions of reactor internals components
- Using those materials properties, to construct an irradiated material–specific constitutive behavior model for use in a finite-element-based analysis methodology for the engineering evaluation and assessment of PWR internals components under long-term reactor operation

Approach

The principal investigators compiled a list of stainless steel material properties from the available literature, documented those properties in MRP-211, and incorporated them in the constitutive modeling of stainless steel material behavior that reflects the PWR operating environment. Additional sources of information used by the principal investigators include experimental data from the industry and the EPRI MRP, including the Reactor Internals Issues Task Group and Joint Owner's Baffle Bolt programs. The correlations and equations delineated in this report are representative of best-fit trends to existing test datasets; however, they are not bounding, and a

statistical assessment of uncertainty has not been performed. Consequently, these correlations and equations are not intended to be used for engineering design calculations. The model is formulated to accept new data as they become available and is constructed for use in a general-purpose finite-element code, with application to both two-dimensional and three-dimensional geometries.

Results

The developed material behavior model, described analytically in this report, is programmed in a user-material subroutine that makes it possible to adapt a commercially available general-purpose finite element computer program to the application of engineering evaluation and assessment of reactor internals. In this way, PWR internals components of various designs are subjected to the same analytical treatment, thereby providing technical uniformity to engineering evaluation and assessment among analysts.

Applications, Value, and Use

The development of the material model presented in this report and its implementation in a component engineering evaluation assessment methodology are essential elements of the industry's reactor internals aging management program.

Keywords

Engineering evaluation and assessment
Finite-element analysis
Functionality
Irradiated stainless steels
Material constitutive model
Pressurized water reactor (PWR) internals components

ABSTRACT

A material constitutive model is developed for irradiated stainless steel Types 316 and 304. The material properties considered in the model include the following basic properties for both stainless steel types: (a) the elastic-plastic properties represented in the complete stress-strain curve—namely, elastic modulus, yield strength, ultimate tensile strength, uniform elongation, and total elongation, expressed as a function of initial cold work, irradiation dose, and temperature; (b) irradiation creep; (c) void swelling; and (d) material failure limits associated with the primary damage mechanisms considered to be potentially operative in stainless steel components in pressurized water reactor (PWR) environments, which include irradiation-assisted stress corrosion cracking and irradiation-induced loss of ductility. The model's database is described in the newly revised MRP-211, Revision 1, report. MRP-211 contains materials properties data found in various forms of the technical literature, including the *ITER Materials Handbook*, which provided reference properties for unirradiated materials. Relevant parts of these data were analyzed for consistency, modified for irradiation effects, and brought into conformance with data generated in the Joint Owner's Baffle Bolt Program.

The primary purpose of this model development is to construct a material-specific constitutive behavior model for use in a finite-element-based analysis methodology for the engineering evaluation and assessment of PWR reactor internals under long-term reactor operation. An analytically, computationally robust material constitutive model is the most critical element in a finite-element based methodology, which, considering the complex nature of the intended application, places great emphasis on the veracity of the model and the quality of the data from which they are derived. The constitutive model described in this report provides nuclear steam supply system analysts with a consistent, well-based theoretical construct that makes it possible to perform engineering evaluation and assessment of bolted and welded connections, employing global and local finite-element models of PWR internals components subjected to plant operating conditions.

Deliverable Number: 3002013216

Product Type: Technical Report

Product Title: Materials Reliability Program: Development of a Material Constitutive Model for Irradiated Austenitic Stainless Steels (MRP-135, Revision 2)

PRIMARY AUDIENCE: Pressurized water reactor (PWR) utility program engineers

SECONDARY AUDIENCE: Utility in-service inspection engineers

KEY RESEARCH QUESTION

The current generation of PWR plants are approaching the end of their respective licensing periods, and multiple plants have already entered periods of extended operation. The nuclear power industry in the United States developed inspection and evaluation guidelines for managing aging degradation in reactor vessel internals. This report describes a material behavior model for irradiated stainless steel Type 316 and Type 304. The model is for use in performing an engineering evaluation and assessment of bolted and welded connections in PWR internal components subjected to plant operating conditions. The model is to be used in a finite-element-based analysis methodology.

RESEARCH OVERVIEW

A framework for implementing an aging management program for PWR internals component items and using inspections and flaw tolerance evaluations to manage age-related degradation issues was developed over the past 10 years. One of the important elements of this framework is to perform an engineering evaluation on the long-term age-related degradation mechanisms. The evaluation leverages a model that considers the effects of temperature, cold work, and irradiation on materials behavior characteristics, including elastic-plastic stress-strain curve, irradiation-enhanced creep (or simply irradiation creep), void swelling, and materials failure limits associated with primary damage mechanisms, such as irradiation-assisted stress corrosion cracking and irradiation-induced embrittlement.

KEY FINDINGS

- Combined with the results of the PWR reactor internals component functionality analysis documented in the MRP-230 series of reports, this report supports the inspection and evaluation guidelines developed in MRP-227.

WHY THIS MATTERS

The research reported results in a numerically based material behavior model, described analytically in this report, and makes it possible to adapt a commercially available general-purpose finite-element computer program to the application of engineering evaluation and assessment of reactor internals.

HOW TO APPLY RESULTS

MRP-135, Revision 2, is a technical basis document and a key reference report supporting MRP-227.

LEARNING AND ENGAGEMENT OPPORTUNITIES

- MRP Assessment and Inspection Technical Advisory Committees (TAC)

EPRI CONTACTS: Kyle Amberge, 704.595.2039, kamberge@epri.com

PROGRAM: Pressurized Water Reactor Materials Reliability Program, P41.01.04

IMPLEMENTATION CATEGORIES: Technical Basis Report, Reference

Together...Shaping the Future of Electricity®

Electric Power Research Institute
3420 Hillview Avenue, Palo Alto, California 94304-1338 • PO Box 10412, Palo Alto, California 94303-0813 USA
800.313.3774 • 650.855.2121 • askepri@epri.com • www.epri.com

SYMBOLS AND ABBREVIATIONS

Symbol	Description	Units
t	time	sec
T	temperature	^{o}C or ^{o}K
φ or d	neutron dose	dpa
E	elastic modulus	GPa
ν	Poisson's Ratio	
ρ	mass density	kg/m^3
α	thermal expansion coefficient	1E-6 m/m-^{o}C
k	thermal conductivity	W/m-^{o}K
Cp	specific heat capacity	J/kg-^{o}K
$\underset{\sim}{\sigma}$	total stress vector	Pa
σ_{ij}	stress component	Pa
$\bar{\sigma}$	effective stress	Pa
S_{ij}	deviatoric stress	Pa
S	volumetric stress	Pa
$\underset{\sim}{\Delta\varepsilon}$	incremental strain vector	m/m
$\Delta\varepsilon_{ij}$	incremental strain component	m/m
Δe	incremental volumetric strain	m/m
Δe_{ij}	incremental deviatoric strain	m/m
$\Delta\bar{e}$	incremental effective strain	m/m
C_{ijkl}	stress-strain matrix	Pa
H_{ijkl}	inverse stress-strain matrix	1/Pa
YS	0.2% yield strength	MPa
UTS	ultimate tensile strength	MPa
UE	uniform elongation	%

Symbol	Description	Units
TE	total elongation	%
CW	cold work ratio	
σ_Y	yield stress at elastic limit	MPa
$\sigma_{0.002}$	yield stress at 0.002 strain	MPa
σ_U	ultimate tensile strength	MPa
$\Delta\sigma_{U-Y}$	$\sigma_U - \sigma_{0.002} = \mathrm{UTS} - \mathrm{YS}$	MPa
$\Delta\sigma_{U-\mathrm{Ye}}$	$\sigma_U - \sigma_Y$	MPa
ε_U	uniform elongation	m/m
ε_T	total elongation	m/m
$\Delta\varepsilon_{T-U}$	$\varepsilon_T - \varepsilon_U$	m/m
$\eta(c)$	cold work factor function	
$\xi(d)$	irradiation factor function	

CONTENTS

LIST OF FIGURES

LIST OF TABLES

1
INTRODUCTION

The cracking of baffle bolts detected in some pressurized water reactor (PWR) plants in recent years has been attributed to an environmentally induced damage mechanism known as *irradiation-assisted stress corrosion cracking* (IASCC). Some of the cracked bolts showed part-through cracks or total failure at relatively low irradiation dose levels (~15 dpa), whereas others of similar material characteristics subjected to similar pre-load, irradiation, and temperature conditions (such as bolts located at symmetric positions around the core) showed no evidence of excessive damage. Materials testing research programs and analytical evaluations of operational conditions have been undertaken by the Reactor Internals Issue Task Group (RI-ITG) within the Electric Power Research Institute's (EPRI's) Materials Reliability Program (MRP) in an effort to identify aging and degradation effects of which irradiation-assisted stress corrosion cracking susceptibility is a possible precursor [1].

Data generated for material performance under irradiation and temperature conditions similar to the baffle bolt environment have identified IASCC as the most likely failure mechanism. A detailed evaluation method is needed to integrate separate effects material test data [2, 3] into a model that permits plant operational conditions to be used to estimate individual bolt response. The development and application of such a model would help quantify material susceptibility to IASCC and consequently develop IASCC susceptibility criteria.

The management of baffle bolt degradation as currently practiced requires that periodic inspection be performed for all the bolts, including the core barrel, at scheduled intervals. However, the current periodic inspection procedures defined in American Society of Mechanical Engineers Boiler and Pressure Vessel Code (ASME B&PV Code) Section XI, which are based on visual examination, could not identify cracking of baffle bolts at the most likely failure locations (such as under the bolt head at the connection to the bolt shank). Because most plants in the United States have already received extensions of their original 40-year licenses to 60 years and are considering license extension to 80 years, a cost-effective inspection strategy supported by analytical guidance would be needed. Additionally, reactor vessel (RV) internals performance under combinations of degraded conditions (that is, their functionality) should be studied. Almost all U.S. nuclear plants require life extension past 60 years to operate beyond 2050.

The development of an analytical methodology for evaluating internals component performance requires the integration of several technical elements—namely, an irradiated material constitutive model, irradiation-induced damage criteria, global and local finite-element models of the internals component assemblies, and plant operating conditions. The material model, which is the most complicated to construct given the current state of knowledge and available data, constitutes the engine that drives the finite-element computational models to produce the stress-strain response for consequent damage evaluation. However, as the only generic element in the analysis methodology, in the sense that it is user-independent and generally applicable to any

plant with similar materials, the material model can be developed as a transferable tool to nuclear steam supply system (NSSS) users to apply to their own finite-element analyses. Thus, by maintaining a consistent approach among NSSS analysts at the material's constitutive level, useful technical exchanges in areas most important to structural performance can be achieved.

The constitutive behavioral regimes considered in the model include elastic-plastic material response considering irradiation hardening of the stress-strain curve, irradiation creep, stress relaxation, and void swelling. IASCC and material embrittlement with irradiation are the primary damage mechanisms considered in the model. Other important damage mechanisms that do not lend themselves to constitutive formulation, such as fatigue and fracture, are not part of this material model. However, they can be evaluated separately using structural analysis results based on the use of the model.

The development of the material's behavior model consists of two parts—(1) the present report, which describes the constitutive relationships based on the EPRI report *Materials Reliability Program: PWR Internals Age-Related Material Properties, Degradation Mechanisms, Models, and Basis Data—State of Knowledge (MRP-211, Revision 1)* [4], and (2) *Irradiated Austenitic Stainless-Steel Constitutive Model (IRADSS) Version 1.0*, which is an executable file cabinet containing a FORTRAN subroutine and installation and user's manual [5]. This capability makes it possible to perform a root-cause analysis of bolt failures and explain the seemingly nonsymmetric damage observed in some plants that is indicative of a nonsymmetric loading environment. An example of such a nonsymmetric loading environment is nonsymmetric temperature distribution, which has two additive effects on bolt response—material constitutive behavior and structural distortion of the whole baffle-former-barrel assembly.

1.1 Purpose

This report is prepared as a tool to assist structural analysts in evaluating the functionality of PWR internals components under long-term reactor operation. The report describes a constitutive model for irradiated stainless steel, mainly types 304 SA and 316 CW, incorporating the latest information on the effects of plasticity, creep, stress relaxation, void swelling, IASCC, and embrittlement as a function of temperature, cold work, and neutron dose.

1.1.1 Scope

Austenitic stainless steel materials are known to have good strength, ductility, toughness, and corrosion resistance. However, when placed in a PWR environment, these properties undergo changes due to long-term neutron exposure, high temperature, reactor water, and loading. Irradiation aging in austenitic stainless steel is characterized by a decrease in ductility and fracture toughness, increase in yield and ultimate tensile strengths, and potential volume changes due to void formation. Under certain conditions of stress, temperature, and neutron damage, irradiated austenitic stainless steel becomes susceptible to IASCC. For service conditions typical of bolted connections in reactor internals structures, irradiation creep and void swelling could combine, under localized gamma heating and irradiation effects, to change the original bolt pre-stress conditions. These interacting regimes must be considered when extracting material property data from the literature for the purpose of constructing a material behavior model.

An analytically robust material behavior model is a critical first step in the damage evolution analysis of aging stainless steel components. The model development takes full advantage of the significant work performed under the RI-ITG program to improve the knowledge of the materials properties of irradiated stainless steels. As part of the RI-ITG program, tests have been conducted to link the separate effects of temperature, neutron damage, cold work, and chemical composition to the changes in stainless steel properties. Microstructural characteristics have been used to help explain the materials properties evolution, identify relevant damage mechanisms, and identify the failure mode when it occurs. Data from these tests have been used to develop materials equations that characterize the yield strength, ultimate tensile strength, uniform elongation, total elongation, reduction in area, void swelling, and irradiation creep of stainless steels in a PWR environment. Although the development of the model's equations has been statistically faithful to the materials database, the correlations and equations delineated in this report are representative of best-fit trends to existing test datasets and are not bounding; a statistical assessment of the uncertainty has not been performed. Consequently, these correlations and equations are not intended to be used for engineering design calculations. However, some approximations were introduced in the relevant sections to ensure appropriate conservatism in the model's application, consistent with accepted engineering practice.

Although it is unlikely that the model's extensive database, which was recently updated in MRP-211, Revision 1 [4], will need to be updated again soon, the model is formulated for ease of expansion to include new data, if necessary. Because the test data and related empirical formulas are reported in the international system of units (SI), the constitutive model has been developed using SI units. Table 1-1 for conversion between SI and English engineering units is included for convenience. The material model is constructed so that it can be applied to both two-dimensional and three-dimensional geometries, easily revised, and adapted to any general-purpose finite element code.

Table 1-1
Conversion table for converting English units to SI units

Physical Quantity	To Convert English Units	Multiply by	To Obtain SI Units
Area	in^2	6.4516E-4	m^2
Burnup	MWd/Mt U	86.4	MW-s/kg U
Chemical Element Concentr.	ppm	1	ppm
Coefficient of Heat Transfer	Btu/hr-ft^2-°F	5.6783	W/m^2-°K
Coef. of Thermal Expansion	ft/ft-°F	1.8	m/m-°K
Creep Compliance Rate	/hr-psi	4.0288E-08	/s-Pa
Density	lb_m/ft^3	16.018	kg/m^3
Enthalpy/Stored Energy	Btu/ lb_m	2325.9	J/Kg
Fast Fluence	n/cm^2	10000	n/m^2
Fast Flux/Linear Heat Rate	n-ft/cm^2-s-kW	3048	n/m-s-kW
Fission Constant	fissions/cm^2-s-kW	10000	fissions/m^2-s-kW

Table 1-1 (continued)
Conversion table for converting English units to SI units

Physical Quantity	To Convert English Units	Multiply by	To Obtain SI Units
Fission Gas Release	%	1	%
Fission Gas Trapped	moles/in^3	61023.7	moles/m^3
Force	lb_f	4.4482	N
Grain Size	microns	1	microns
Heat/Energy	Btu	1055	J
Heat Flux	Btu/hr-ft^2	3.1525	W/m^2
Length	in	0.0254	m
Linear Heat Rate	kW/ft	3.2808	kW/m
Mass	lb_m	0.45359	kg
Mass Flow Rate	lb_m/hr	1.25997E-04	kg/s
Mass Flux	lb_m/hr-ft^2	1.35622E-03	kg/s-m^2
Neutron Flux	n/cm^2-s	10000	n/m^2-s
Oxide Thickness	mils	25.4	microns
Power	Btu/hr	0.29288	W (J/s)
Pressure/Stress	psi	6894.8	Pa (N/m^2)
Specific Heat	Btu/lb_m-°F	4186.5	J/kg-°K
Specific Volume	ft^3/lb_m	6.24280E-02	m^3/kg
Spring Constant	lb_f/ft	14.594	N/m
Strain	ft/ft	1	m/m
Strain Energy Density	Btu/ft^3	37250	J/m^3
Surface Roughness	mils	25.4	microns
Temperature	°F	(°F-32)/1.8+273.15	°K
Temperature Rate	°F/hr	1.543E-04	°K/s
Thermal Conductivity	Btu/hr-ft-°F	1.7296	W/m-°K
Time	hr	3600	s
Velocity	ft/hr	8.46670E-05	m/s
Viscosity	lb_f-hr/ft^2	1.72369E+05	N-s/m^2
Volume	in^3	1.63870E-05	m^3
Volume Heating	Btu/hr-ft^3	10.343	W/m^3

Table 1-1 (continued)
Conversion table for converting English units to SI units

Physical Quantity	To Convert English Units	Multiply by	To Obtain SI Units
Volume Rate	in^3/hr	4.552E-09	m^3/s
Weight Gain	lbm/in^2	703.07	kg/m^2

This report covers the constitutive model development in some detail. Section 2 presents an overview of the factors that must be considered before a constitutive model is formulated. Section 3 describes modeling details, which include the assumptions and limitations used in the model's formulation and materials property equations and their plots. Section 4 lists the references.

2
GENERAL OVERVIEW

Mechanical failures in PWR core support structures are sometimes difficult to diagnose because they involve a complex interaction of load, time, and environmental conditions that include temperature, radiation, and corrosion. Furthermore, the temperature and neutron flux are nonuniform, and applied loads can be monotonic, steady, transient, cyclical, and multiaxial. The forensic failure analysis of RVs' internals components based on all of these factors is nontrivial.

To illustrate this point, studies have been conducted in the past few years to explain why baffle/former bolts crack. No definitive failure pattern has emerged from the studies, although locations of high stress, neutron dose, and temperature appear to be more susceptible. The failed bolts usually exhibit low ductility, and they fail in the region of high strain concentration under the bolt head near the shank. This general behavior can best be evaluated by incorporating the developed constitutive model in a detailed finite-element analysis procedure that faithfully represents the loading and physical environment of the structural system being analyzed. Understanding the structure's loading and environmental conditions is critical to prescribing the correct analysis procedure. This section presents a brief discussion of those conditions.

2.1 PWR Loads and Environment

RV internals are designed to withstand steady and fluctuating forces that could be present during normal operation and accident conditions, considering predefined mechanical properties that might not reflect aging-related effects. However, the combined effects of the operating environment, such as neutron irradiation, elevated temperatures, and exposure to the primary coolant, can have a significant impact on the assessment and management of the RV internals' aging [6, 7]. *Aging* is defined as the cumulative changes over time that can impair the ability of a component to function within accepted criteria. An aging mechanism is any process that gradually changes the characteristics of a component with time and use. Operating conditions that exceed prescribed limits can accelerate the degradation rate. Loads can influence aging mechanisms through changes in stresses caused by changes in temperature, radiation, and oxidizing environments.

2.1.1 Loads on PWR RV Internals

Steady-state loads originate from pressure differences, temperature gradients, and mechanical loads. Cyclic loads are classified as system cycling, thermal cycling, or flow-induced vibration.

System cycling is caused by changes in the pressure and temperature within the reactor. Events such as startup, shutdown, scram, and safety/relief valve blowdown are typical examples.

Temperature fluctuations are categorized as thermal cycling. Temperature transients can create local and global temperature gradients at material interfaces. These transients are classified as slow or rapid. Slow thermal cycling is exemplified by events such as reactor startup, reactor shutdown, or load-following operation mode. Rapid thermal cycling is associated with connection or disconnection of systems, emergency core cooling system water injection, or leakage of hot or cold water into the system.

Flow-induced vibrations are cyclic loads produced by turbulence, pump excitation, and vortices shedding from an RV internals component as coolant flows by.

RV internals components can be subjected to fatigue damage by system cycling, but the ASME Code design allowances for it are generally adequate, provided that the transients are known. The aging mechanism of thermal cycling is generally low cycle fatigue, whereas that for flow-induced vibration is high cycle fatigue. In addition, the RV internals components can be subjected to seismic and loss-of-coolant-accident blowdown loads, which can challenge the functionality requirements of these components. Although design basis loads do not participate in the aging mechanisms, they constitute the ultimate test of whether the degradation has progressed to an unacceptable level in the presence of transient loads.

2.1.2 PWR Temperatures and Neutron Irradiation

RV internals components are exposed to strong temperature and neutron irradiation gradients, depending on their location relative to the reactor core and the power distribution, producing nonuniform distributions of temperature and neutron flux in the core's surrounding structures. The temperatures can range from 270°C to 340°C. The lowest temperatures occur in the core barrel, and the highest temperatures (outside the core itself) occur in the baffle/former plates and bolts closest to the reactor core. When gamma heat generation is added, the temperatures will be higher. For example, the peak temperature could be as high as approximately 400°C locally due to gamma heating. The neutron dose varies over a wide range during the life of the plant. The highest neutron dose also occurs in the baffle/former plates and bolts. Table 2-1 [6, 7] summarizes the temperatures and neutron dose at 32 effective full-power years of operation (EFPY) in PWRs. The magnitudes of the neutron dose listed in Table 2-1 are only representative values because strong gradients in neutron dose exist. The neutron flux varies axially, radially, and circumferentially. It also varies with time because irradiation conditions vary with assembly-wide core power distributions, burnup of fuel assemblies, core loading patterns, addition of neutron absorbers, and so on. Nevertheless, Table 2-1 gives a general overview of the operating conditions for a PWR.

Table 2-1
Representative operating conditions of PWRs

		Estimated at 32 EFPY		
		Fluence (10^{21} n/cm^2)		
Plant Component	**Temperature (°C)**	**E>0.1 MeV**	**E>1 MeV**	**dpa**
U.S. 900-MW NPP				
Core barrel	—	18	6.9	12
Core baffle	—	160	74	110
Formers	—	18–160	7–74	12–110
Bolts	—	160	74	110
Upper core plate	—	0.43	0.22	0.3
Lower core plate	—	6.2	3.2	4.6
French 900-MW NPP				
Core barrel	286–320	14	7	9.6
Core baffle	290–370	109	54	80
Formers	290–370	13–76	6–38	10–56
Bolts	300–370	82	41	58
Upper core plate	—	0.5	0.25	0.3
Lower core plate	—	3–8	1.5–4	2–5.6
French 1300-MWe NPP				
Core barrel	290–328	—	~3	~3.6
Core baffle	~328	—	~11	~13
German Konvoi 1300-MWe NPP				
Core baffle (barrel)	~325	1.4	0.8	1.2
Core envelope (shroud)	~325	106	50	75
Bolts	~325	—	—	—
Upper core plate	~325	0.48	0.3	0.45
Lower core plate	~290	0.17	0.11	0.17

Note: 15 dpa ≈ 10^{22} n/cm^2, E > 1 MeV

7 dpa ≈ 10^{22} n/cm^2, E > 0.1 MeV

2.2 Finite-Element Analysis with User-Defined Material Subroutine

Material models found in general-purpose finite-element codes are inadequate for the analysis of aging degradations of stainless steel components in a PWR environment. The reactor core internals require a material constitutive model that allows the material's behavior to vary with temperature, strain rate, neutron flux, and neutron dose. In addition, the model needs to include rate processes such as irradiation creep, stress relaxation, and irradiation growth due to void swelling. To allow the use of such a model in finite-element analysis, the finite-element code

must provide the capability to access a user-defined material model. ABAQUS[1] and ANSYS[2] are finite-element codes that allow the specification of user-defined material subroutines, which are linked to the code as UMAT for ABAQUS and as USERMAT for ANSYS. The FORTRAN package IRADSS [5] is constructed as a host-code independent material subroutine, which can be linked to either ANSYS or ABAQUS as previously described.

2.2.1 ANSYS-IRADSS Solution Procedure

ANSYS solves nonlinear problems using an incremental procedure. This procedure approximates a nonlinear problem as a series of piecewise linear problems (that is, steps). An iterative scheme is used to solve for the incremental displacement at each step. For weakly nonlinear problems, a single iteration per step could be sufficient. However, for strongly nonlinear problems, multiple iterations might be required at each step. For iterations within a step, a (tangent) stiffness matrix and incremental load vector are constructed, and a trial set of incremental displacements are found. ANSYS continues to iterate within a step until the unbalanced forces and the displacement corrections are small or until it reaches preset solution limits (for example, convergence). When the IRADSS material subroutine is used, the process is the same. The only difference is that ANSYS passes solution information to the user subroutine for reconstruction of the tangent stiffness matrix and incremental load vector. This information includes time, temperature, strains, and stresses at the start of the increment; the change in time, temperature, and strains for the current increment; and other data. Other information, such as total neutron dose and total plastic strain, can be stored in user-defined state variables. For each increment, IRADSS calculates the current material properties, current stress-strain matrix, and stresses at the end of the increment. ANSYS uses the calculated stresses to determine the force imbalance and iterates until the solution converges.

2.2.2 Constitutive Formulation Procedure

The constitutive formulation procedure for the stainless steel described in this report and incorporated in IRADSS is listed in the following as a series of steps. For each step, there is a brief description and a list of equations calculated in that step. The equations are written in indicial notation. Stresses and strains are defined in terms of six components of stress and strain for generality. Fewer components are needed for one-dimensional and two-dimensional elements. Small strain theory for viscoplastic materials is assumed. Thermal creep and oxide growth are assumed to be small and will be ignored in the following discussion.

In the following equations, $\sigma_{ij} = S_{ij} + S\,\delta_{ij}$ and $\Delta\varepsilon_{ij} = \Delta e_{ij} + \Delta e\,\delta_{ij}$, where σ_{ij} = total stress component, S_{ij} = deviatoric stress components, S = volumetric stress, $\Delta\varepsilon_{ij}$ = total incremental strain, Δe_{ij} = incremental deviatoric strain, Δe = incremental volumetric strain, and δ_{ij} is the Kronecker delta, where δ_{ij}=1 when i=j and zero otherwise. The materials properties are assumed to be constant for the increment and are evaluated at the middle of the increment. Strain rate is the average strain rate for an increment. All other variables are evaluated at the end of the increment unless noted otherwise. For example, ${}^{t}\sigma$ is the stress at the start of the increment, and ${}^{t+\Delta t}\sigma$ is the stress at the end of the increment.

[1] ABAQUS is a registered trademark of Dassault Systèmes.
[2] ANSYS is a registered trademark of ANSYS, Inc.

The steps are as follows:

1. Get the previous total stress and current incremental strain vectors:

$${}^{t}\sigma = \{\sigma_{11}\ \sigma_{22}\ \sigma_{33}\ \sigma_{12}\ \sigma_{13}\ \sigma_{23}\}$$ Total stress vector

$$\Delta \underset{\sim}{\varepsilon} = \{\Delta\varepsilon_{11}\ \ \Delta\varepsilon_{22}\ \ \Delta\varepsilon_{33}\ \ 2\Delta\varepsilon_{12}\ \ 2\Delta\varepsilon_{13}\ \ 2\Delta\varepsilon_{23}\}$$ Incremental strain vector

2. Get material properties for the current time increment. The properties at a given cold work ratio are evaluated at the temperature, neutron flux, and neutron dose at the middle of an increment. (Note that the cold work ratio for solution-annealed stainless steel is zero.) The thermal strain and irradiation growth due to both void swelling and irradiation creep are calculated at the end of the increment. The material property equations are shown in Section 3.

3. Define the stress-strain matrix, $\underline{C}$, and its inverse, $\underline{H}$:

$$\Delta\sigma_{ij} = C_{ijkl}\,\Delta\varepsilon_{kl}$$ Incremental stress-strain relation

$$\Delta\varepsilon_{ij} = H_{ijkl}\,\Delta\sigma_{kl}$$ Inverse stress-strain relation

4. Assume additive decomposition of strain rates (scalar − valued):

$$\dot{\bar{e}} = \dot{\bar{e}}^{E} + \dot{\bar{e}}^{C_{irr}} + \dot{\bar{e}}^{C_{th}} + \dot{\bar{e}}^{P}$$ Total effective strain rate

$$\dot{\bar{e}}^{E}$$ Effective elastic strain rate

$$\dot{\bar{e}}^{C_{irr}}$$ Effective irradiation creep rate

$$\dot{\bar{e}}^{C_{th}} << \dot{\bar{e}}^{C_{irr}}$$ Effective thermal creep rate (ignored)

$$\dot{\bar{e}}^{P}$$ Effective plastic strain rate

5. Calculate the total incremental strain for small strains and small deflections:

$$\Delta\varepsilon_{ij} = \Delta\varepsilon_{ij}^{E} + \Delta\varepsilon_{ij}^{TH} + \Delta\varepsilon_{ij}^{V} + \Delta e_{ij}^{C_{irr}} + \Delta e_{ij}^{C_{th}} + \Delta e_{ij}^{P}$$

$$\Delta\varepsilon_{ij}^{E}$$ Elastic strain components

$$\Delta\varepsilon_{ij}^{TH} = \Delta\varepsilon^{TH}\delta_{ij}$$ Thermal strain increment (see Eqs. 3-21 to 3-23)

$$\Delta\varepsilon_{ij}^{V} = \Delta\varepsilon^{V_{irr}}\delta_{ij}$$ Irradiation growth (void swelling) (see Eq. 3-27)

$$\Delta e_{ij}^{C_{irr}} = \Delta\varepsilon_{ij}^{C_{irr}}$$ Irradiation creep strain increment (see Eq. 3-31)

$$\Delta e_{ij}^{C_{th}} = \Delta\varepsilon_{ij}^{C_{th}} << \Delta\varepsilon_{ij}^{C_{irr}}$$ Thermal creep strain increment (ignore)

$$\Delta e_{ij}^{P} = \Delta\varepsilon_{ij}^{P}$$ Plastic strain increment

$$\delta_{ij} = 1 \text{ for } i = j;\ = 0 \text{ for } i \neq j$$ Kronecker delta

6. Remove non-stress-producing strains from the incremental strain vector:

$$\Delta\varepsilon_{ij}^{'} = \Delta\varepsilon_{ij} - \Delta\varepsilon^{th}\delta_{ij} - \Delta\varepsilon^{V_{irr}}\delta_{ij}$$

7. Calculate the volumetric, deviatoric, and effective strain for the current increment:

$\Delta e^{'} = \frac{1}{3}\,\Delta\varepsilon^{'}_{kk}$ Incremental volumetric strain

$\Delta e_{ij} = \Delta\varepsilon^{'}_{ij} - \Delta e^{'}\delta_{ij}$ Incremental deviatoric strain component

$\Delta\bar{e} = \sqrt{\frac{2}{3}\Delta e_{ij}\Delta e_{ij}}$ Incremental effective strain increment

8. Calculate the volumetric, deviatoric, and effective stresses at the start of the increment:

${}^{t}S = \frac{1}{3}{}^{t}\sigma_{kk}$ Volumetric stress

${}^{t}S_{ij} = {}^{t}\sigma_{ij} - {}^{t}S\delta_{\mathrm{ij}}$ Deviatoric stress

${}^{t}\bar{\sigma} = \sqrt{\frac{3}{2}{}^{t}S_{ij}\,{}^{t}S_{ij}}$ von Mises effective stress

9. Calculate irradiation effective creep strains:

$\Delta\bar{e}^{C_{irr}} = \dot{\bar{e}}^{C_{irr}}\Delta t$ Irradiation creep strain increment

$\Delta\bar{e}^{C} = \Delta\bar{e}^{C_{irr}}$ Total creep strain increment

$\Delta\bar{e}^{inelastic} = \Delta\bar{e}^{C} + \Delta\bar{e}^{P}$ Total inelastic strain increment

10. Calculate the creep strain components from the Flow Rule:

$de^{C}_{ij} = \lambda\frac{\partial F}{\partial\sigma_{ij}} = 3\lambda S_{ij},\ \lambda = \frac{1}{2}\frac{\Delta\bar{e}^{C}}{{}^{t}\bar{\sigma}}$ Flow Rule

$F = \left[\frac{1}{2}{}^{t}S_{ij}\,{}^{t}S_{ij} - \frac{1}{3}\sigma_{y}^{2}\right] = 0$ von Mises yield criteria

$\Delta e^{C}_{ij} = \Delta\bar{e}^{C}\left(\frac{3}{2}\frac{{}^{t}S_{ij}}{{}^{t}\bar{\sigma}}\right) = \Delta\bar{e}^{C}n_{ij}$ Creep strain components

11. Remove creep strains from incremental deviatoric strains:

$\Delta\mathrm{e}^{'}_{\mathrm{ij}} = \Delta\mathrm{e}_{\mathrm{ij}} - \Delta\mathrm{e}^{C}_{\mathrm{ij}}$

12. Calculate the stress at the end of the increment:

${}^{t+\Delta t}\sigma_{ij} = {}^{t}\sigma_{ij} + C_{ijkl}\Delta e^{'}_{kl}$

13. Calculate the volumetric, deviatoric, and effective stress at the end of the increment:

${}^{t+\Delta t}S = \frac{1}{3}{}^{t+\Delta t}\sigma_{kk}$ Volumetric stress

${}^{t+\Delta t}S_{ij} = {}^{t+\Delta t}\sigma_{ij} - {}^{t+\Delta t}S\delta_{ij}$ Deviatoric stress

${}^{t+\bar{\Delta}t}\sigma = \sqrt{\frac{3}{2}{}^{t+\Delta t}S_{ij}\,{}^{t+\Delta t}S_{ij}}$ von Mises effective stress

14. Calculate the yield stress for current temperature, neutron dose, and cold work:

$\sigma_y = \sigma_y(T, \varphi(T), \varphi)$ Yield stress with strain hardening

15. Scale the stresses using radial return if the effective stress exceeds the yield stress:

$R = \frac{\sigma_y}{t+\bar{\Delta}t_\sigma}$ where, ${}^{t+\bar{\Delta}t}\sigma \geq \sigma_y$ Radial return factor

${}^{t+\Delta t}\sigma_{ij}' = R\ {}^{t+\Delta t}\sigma_{ij}$ Total stress predicted

$\Delta e_{ij}^P = H_{ijkl}\,{}^{t+\Delta t}\sigma_{kl}(1-R)$ Incremental plastic strain components

$\Delta e_{ij}^E = \Delta e_{ij} - \Delta e_{ij}^P$ Incremental elastic strain components

16. Save the material state at the end of the increment in user-defined state variables.

Figure 2-1 shows how the stress increment, $\Delta\sigma$, is calculated for a strain increment, $\Delta\varepsilon$. The stress and strain shown in Figure 2-1 are the effective stress and strain in the von Mises sense, that is, they are the uniaxial equivalent of a multi stress-strain state. The stress increment is first estimated by using the elastic stress-strain constitutive matrix. The total effective stress at the end of the increment is then compared to the yield stress for the increment. If the effective stress exceeds the yield stress, the radial return factor, *R*, is used to scale the effective stress to the yield surface. The plastic part of the strain increment is $(1\text{-}R)\ {}^{t+\Delta t}\sigma/E$. The elastic part is $\Delta\varepsilon - \Delta\varepsilon^P$.

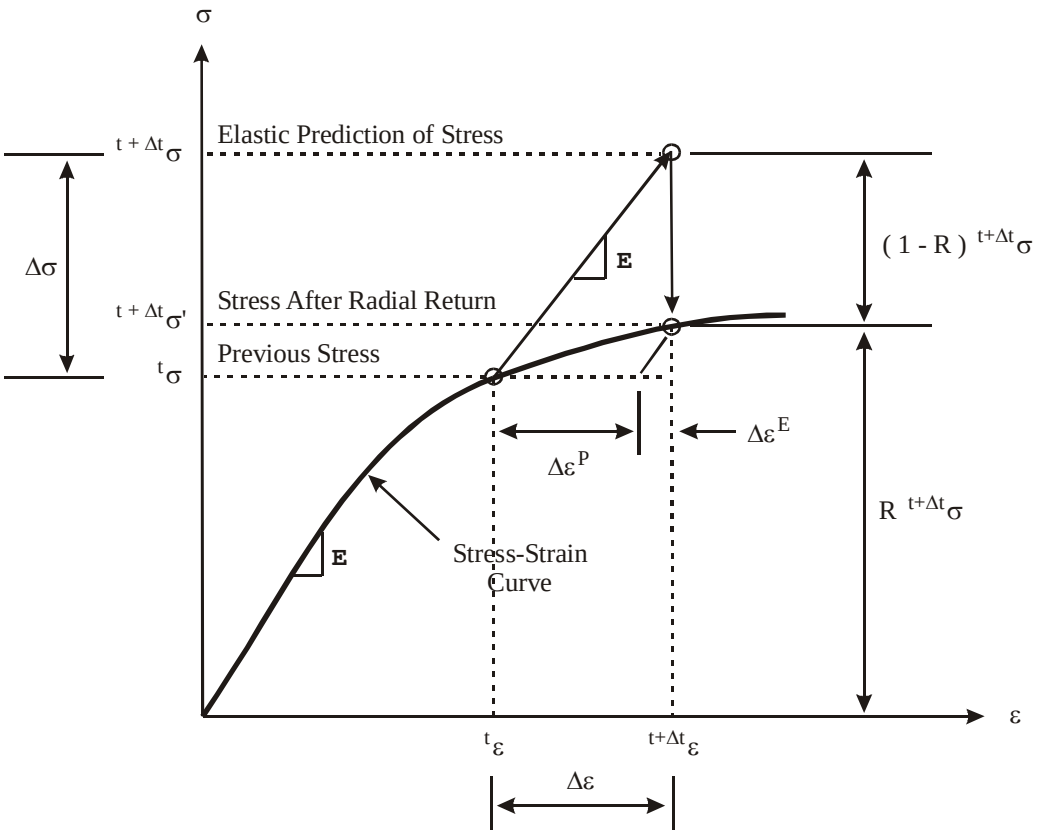

Figure 2-1
Incremental stress-strain relation

3
CONSTITUTIVE PROPERTIES FOR AUSTENITIC STAINLESS STEEL

3.1 General Description of Model

A generic constitutive model for austenitic stainless steel subjected to PWR environmental conditions has been developed. This generic model is intended mainly for Type 316 and 304 stainless steel exposed to high neutron irradiation, high temperature, and PWR water conditions. It is a working model that includes the essential features of irradiated material. This working model can be used for the engineering evaluation and assessment of PWR RV internals under long-term operational conditions, considering the separate effects of interactions between irradiation hardening, void swelling, irradiation creep, and plasticity.

3.2 Assumptions and Limitations

Use of the material model is limited to typical PWR conditions as described in Section 2. The reactor vessel internal components in a typical PWR are generally exposed to temperatures that range from 270°C to 370°C and neutron dose rate per year ranging from less than 0.2 dpa to over 2.4 dpa. The RV internals components are also exposed to strong gradients in temperature and neutron flux. The applied loads may be steady-state and/or cyclic. Cyclic loads are assumed to be quasi-static. The constitutive model is intended for evaluating the performance of RV internal components under normal, long-term reactor operations. Under these conditions, high strain rate loading or excessive plastic deformation are not anticipated. The assumptions for the generic constitutive model are as follows:

- Materials properties are assumed to be isotropic for all unirradiated, annealed Type 300 series stainless steels. Cold work and radiation produce differences in the properties for the different types of stainless steel as a function of the amount of cold work or neutron dose. The materials properties are also assumed to be isotropic for a given amount of cold work or neutron dose.
- Because impact loading causing high strain rates is not anticipated for this application, the materials properties do not include strain rate effects.
- Small strain theory is assumed because excessive plastic straining is not anticipated under normal operating conditions. Thus, engineering stress-strain relations are used in the formulation. Displacements and rotations are small. Strain rate decomposition is additive.
- Elastic modulus is weakly dependent on void swelling, which is a function of temperature and dose, but Poisson’s ratio and mass density are functions of temperature only.

- Plastic behavior is modeled as isotropic hardening. The model is intended for applications where the internals are cycled between operating conditions and shutdown, that is, small plastic straining but no reverse loading into the plastic regime. Under these conditions, there is very little difference, numerically, between kinematic and isotropic hardening, and isotropic hardening is considered adequate.
- Yield strength is based on von Mises yield criteria.
- Plastic behavior is rate-independent, except for irradiation creep. Viscoplastic behavior is modeled as irradiation creep only. Thermal creep is much smaller than irradiation creep and is ignored.
- Thermal expansion and void swelling are isotropic and are treated as volumetric strains, following standard practice in computational mechanics.
- Yield strength and ultimate tensile strength are functions of stainless steel grade, temperature, neutron dose, and cold work.
- The stress-strain curves are defined by the elastic modulus, yield strength, ultimate tensile strength, uniform elongation, and total elongation. The engineering stress-strain curve is used as an approximation for the true stress-strain curve as covered below; however, the material constitutive model in Section 2 is cast in the true-stress-true-strain framework.
- The failure criteria for stainless steel are limited to the onset of IASCC, embrittlement due to excessive void swelling, and stresses and strains that exceed the material mechanical limits (ultimate tensile strength or total elongation). However, application of the failure criteria, using the response variables that correspond to the material's failure limits, is performed as a post-processing activity.

3.3 Types of Stainless Steels Modeled

The constitutive model is currently developed for Types 304 and 316 stainless steels. The material composition for standard grades of these stainless steels is shown in Table 3-1 [8, 9].

Table 3-1
Composition of standard grades of wrought stainless steels

	Chemical Composition, wt%								
Type No.	**Cr Limits**	**Ni Limits**	**C (max)**	**Mn (max)**	**Si (max)**	**S (max)**	**P (max)**	**Mo**	**m**
304	18–20	8–12	0.08	2	1	0.03	0.045		
304L	18–20	8–12	0.03	2	1	0.03	0.045		
316	16–18	10–14	0.08	2	1	0.03	0.045	2–3	
316L	16–18	10–14	0.03	2	1	0.03	0.045	2–3	
347	17–19	9–13	0.08	2	1	0.03	0.045		>10x %C, Cb-Ta

Welded stainless steel material, including irradiation effects, can be modeled as wrought stainless steel with initial residual stresses.

3.4 Construction of the Stress-Strain Curve

The constitutive formulation described in Section 2 constructs valid stress-strain matrix-coefficients C_{ijkl}. These coefficients, which relate the incremental stresses $\Delta\sigma_{ij}$ to the incremental strains $\Delta\varepsilon_{kl}$, are derived from the uniaxial stress-strain curve, generalized for isotropic material as an effective-stress versus effective-strain relationship, which is fundamental to the constitutive formulation process. Construction of the uniaxial stress-strain curve from the mechanical properties is described in this section. The mechanical properties needed for this construction include the elastic modulus, yield strength (elastic limit), 0.2% offset yield strength, ultimate tensile strength, uniform elongation, and total elongation, all as a function of temperature, irradiation dose, and cold work.

An example of the stress-strain behavior of irradiated stainless steel is depicted in Figure 3-1 [10]. If the yield point dip and the curve beyond the uniform elongation are ignored, the stress-strain curves have approximately the same shape, except that the yield strength increases, and the difference between the ultimate tensile strength and yield strength decreases with increasing irradiation dose. Eventually, the difference between the ultimate tensile strength and the yield strength approaches zero at higher neutron doses. The uniform elongation and total elongation are decreasing with increasing neutron dose, as depicted in Figure 3-1. This type of behavior is reproduced in the derivations that follow.

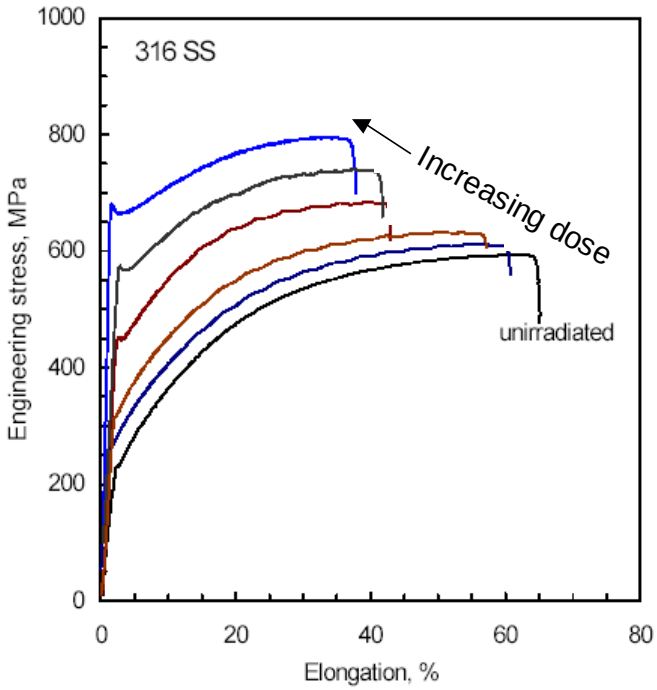

Figure 3-1
Stress-strain curves for various neutron doses for 316 SS [10]

Figure 3-2 shows a schematic of the stress-strain curve, with the upper graph in Figure 3-2 representing an engineering stress-strain curve from a typical test. The shape of this curve is representative of room-temperature stress-strain curves for unirradiated, annealed 316 stainless steel materials [11]. In Figure 3-2, the stress-strain curve is divided into an elastic portion and a plastic portion—line *0-a* is the elastic portion, and line *b-e* is the plastic portion. The plastic

portion can be further divided into a strain-hardening part (line *b*-*d*) and a strain-softening part (line *d*-*e*). The yield strength (σ_Y), ultimate tensile strength (σ_U), and rupture strength (σ_R) correspond to points *a*, *d*, and *e*, respectively. The uniform elongation (ε_U) and total elongation (ε_T) correspond to the strains at the ultimate tensile strength and the rupture strength, respectively. It is noted that the term *uniform elongation* as used in this report is an analytical definition and is the elastic + plastic engineering strain at ultimate tensile strength (see Figure 3-2).

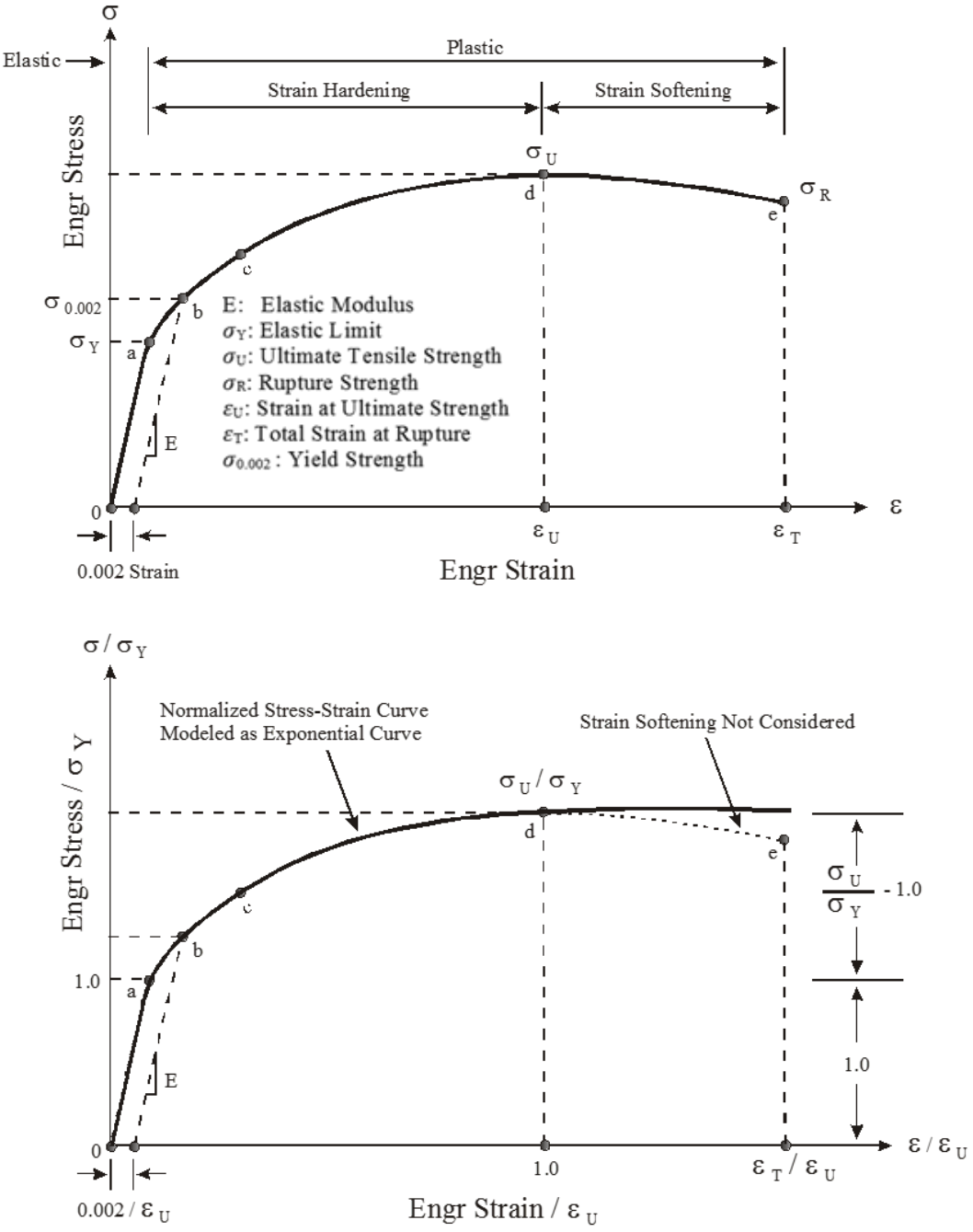

Figure 3-2
Engineering and normalized stress-strain curves

When creating a stress-strain model for large strain analysis, the engineering stresses and strains are usually converted to true strains (logarithmic strains) and true stresses (Cauchy stresses). These data are then fitted to a power law equation. However, the deviation of the true stress-strain curve from the engineering stress-strain curve is small in the strain range expected in PWR internals components (less than 5%), making this conversion unnecessary. Instead of a power law fit, the stress-strain data are fitted to an exponential function of the following form:

$$\boldsymbol{\sigma = \sigma_Y + (\sigma_U - \sigma_Y)[1 - exp(-(\varepsilon - \sigma_Y/E)/\varepsilon_o)], \sigma > \sigma_Y} \qquad \textbf{Eq. 3-1}$$

The variables in Equation 3-1 are defined as follows, with reference to Figure 3-2:

σ_Y = Yield strength at the elastic limit (MPa)

σ_U = Ultimate tensile strength (MPa)

E = Elastic modulus (MPa)

$$\varepsilon_0 = -\ (\varepsilon_c - \sigma_Y/E)\ /\ \log_e[1 - (\sigma_c - \sigma_Y)/\ (\sigma_U - \sigma_Y)],\quad \sigma_b \le \sigma_c \le \sigma_d$$

where ε_c, σ_c are the strain and stress at point *c* used to define ε_o as described in the following.

Note that ε_o is a "shape" parameter for the exponential fit and has a fixed value. This value is determined by evaluating Equation 3-1 using stress and strain values from a known curve having the desired shape. The stress-strain curve is fitted to points *a*, *c*, and *d* shown in Figure 3-2. Point *a* is located at the yield strength or the elastic limit, and point *d* at the ultimate tensile strength. Point *c* is a point that is selected to match the shape of the curve between points *a* and *d*. Point *e* is the point located at the rupture strength. The yield stress data, called the *0.2% yield stress* ($\sigma_{0.002}$), are the stresses resulting in 0.2% plastic strain in the specimens and correspond to point *b* in Figure 3-2. The stress at the elastic limit (σ_Y), needed in the analytical stress-strain relation, can now be estimated from the following equation:

$$\boldsymbol{\sigma_Y = \sigma_U - (\sigma_U - \sigma_{0.002})/\, exp(-0.002/\varepsilon_o)} \qquad \textbf{Eq. 3-2}$$

The stress parameters on the right consider the effects of cold work, temperature, and neutron dose. The stress-strain curve depicted schematically in Figure 3-2 and the stress and strain quantities shown in the figure depend on temperature, irradiation, and cold work. Functional relationships for these quantities are described in sections to follow.

3.4.1 Basic Properties of Unirradiated, Annealed Type 300 Series Stainless Steel

Unirradiated materials properties from the *ITER Materials Handbook* [12] are used as reference properties. Dealing first with the thermal properties, the effect of temperature is derived in the form of a polynomial as shown in Equation 3-3, where T is the temperature in degrees Celsius:

$$\boldsymbol{Property = C_0 + C_1 T + C_2 T^2 + C_3 T^3} \qquad \textbf{Eq. 3-3}$$

The coefficients for the basic thermal property equations are summarized in Table 3-2.

Table 3-2
Thermal property equations for Type 300 series stainless steel

Property	Units	Property = $C_0 + C_1T + C_2T^2 + C_3T^3$; T in °C			
		C_0	C_1	C_2	C_3
Mass density	Kg/m^3	8040.3	-0.44165	0.00002071	-5.8048E-08
Thermal conductivity	W/m-K	13.28571	0.01756205	-5.3788E-06	4.29293E-09
Specific heat capacity	J/kg-K	456.2817	0.4337	-0.00057714	3.5074E-07
Thermal expansion:					
Based on ITER [12]					
Strain ε_{TH}^{ITER}	m/m	-.3520E-03	1.6831E-05	3.6404E-09	-2.3028E-14
Coefficient α_{se}^{ITER}					
Based on ASME [13]:	1E-6/°C	-3.8372E-04	0.0049348	-1.6585E-06	
Strain ε_{TH}^{ASME}	m/m	16.3153	1.6209E-05	5.1300E-09	-1.3714E-12

Note: $\alpha \equiv \alpha_{se}(T)$, the secant coefficient of thermal expansion

Table 3-3 lists the materials property equations for 0.2% yield strength, ultimate tensile strength, uniform elongation, and total elongation for unirradiated, annealed stainless steel. Tables 3-4 and 3-5 include the same information as Table 3-3, except for the 0.2% yield strength, ultimate tensile strength, uniform elongation, and total elongation of Type 316 and Type 347, respectively, which have different coefficients. These properties were derived from Type 300 series stainless steel tests and will be used as the baseline properties for unirradiated, annealed Type 300 series stainless steels in the constitutive model. To visually illustrate the temperature dependence described by Equation 3-3, plots of selected thermal-mechanical properties are shown in Figures 3-3 through 3-9.

Table 3-3
Materials property equations for unirradiated, annealed Type 304 series stainless steel

Property	Units	Property = $C_0 + C_1T$; (T is in °C)		
		C_0	C_1	
Elastic modulus	GPa	200.3795	-0.08122	
Poisson's ratio		0.2921	0.000072	
Property	**Units**	**Property = $C_0 + C_1$*exp(-C_2*T); (T is in °C)**		
		C_0	C_1	C_2
0.2% yield strength	MPa	210.5556	152.4808	0.0345
Ultimate tensile strength	MPa	437.4983	216.1872	0.0135
Uniform elongation	%	21.716	35.3681	0.0064
Total elongation	%	12.4542	58.0042	0.0023

Note: The elastic modulus also depends on void swelling, which is described in Equation 3-28.

Table 3-4
Materials property equations for unirradiated, annealed Type 316 series stainless steel

Property	Units	Property = $C_0 + C_1T$; (T is in °C)		
		C_0	**C_1**	
Elastic modulus	GPa	200.3795	-0.08122	
Poisson's ratio		0.2921	0.000072	
Property	**Units**	**Property = $C_0 + C_1$*exp(-C_2*T); (T is in °C)**		
		C_0	**C_1**	**C_2**
0.2% yield strength	MPa	205.2528	127.8804	0.0075
Ultimate tensile strength	MPa	490.4348	115.9407	0.009
Uniform elongation	%	16.6776	35.64	0.0045
Total elongation	%	23.5217	39.1379	0.0038

Note: The elastic modulus also depends on void swelling, which is described in Equation 3-28.

Table 3-5
Materials property equations for unirradiated, annealed Type 347 series stainless steel

Property	Units	Property = $C_0 + C_1T$; (T is in °C)		
		C_0	**C_1**	
Elastic modulus	GPa	200.3795	-0.08122	
Poisson's ratio		0.2921	0.000072	
Property	**Units**	**Property = $C_0 + C_1$*exp(-C_2*T); (T is in °C)**		
		C_0	**C_1**	**C_2**
0.2% yield strength	MPa	269.75	181.7881	0.0561
Ultimate tensile strength/yield strength	MPa	393.1417	238.1534	0.0102
Uniform elongation	%		42.4554	0.0027
Total elongation	%	30.5842	46.0043	0.0085

Note: The elastic modulus also depends on void swelling, which is described in Equation 3-28.

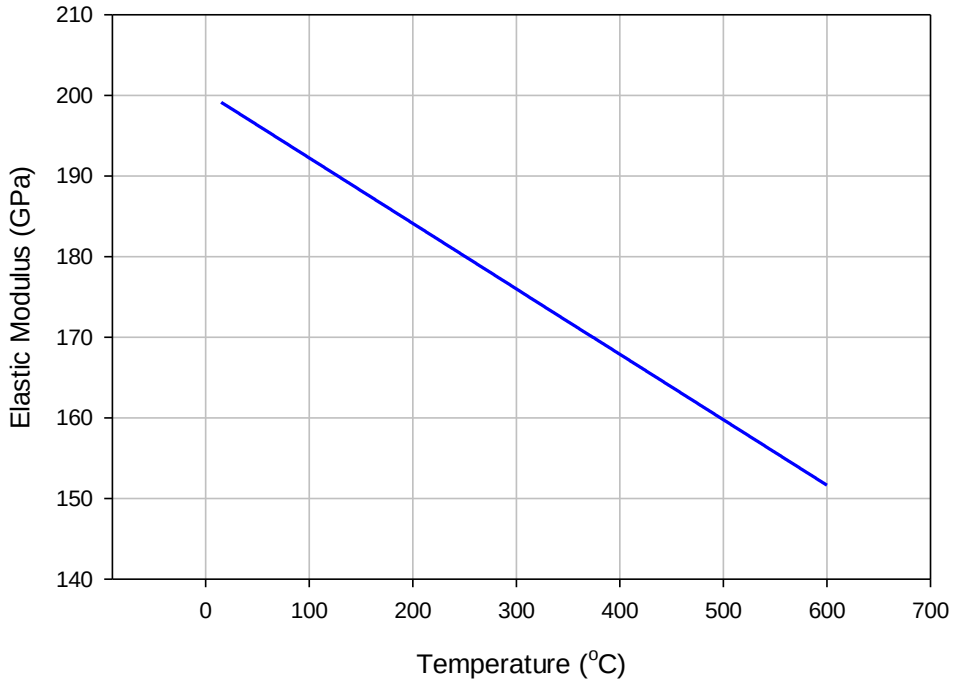

Figure 3-3
Elastic modulus versus temperature for Type 300 series stainless steel

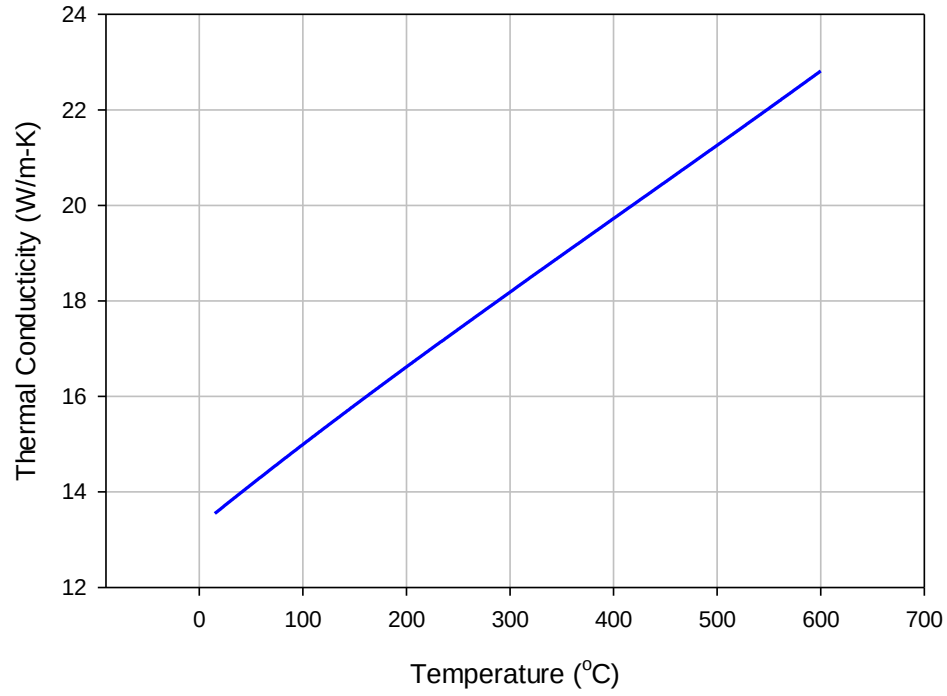

Figure 3-4
Thermal conductivity versus temperature for Type 300 series stainless steel

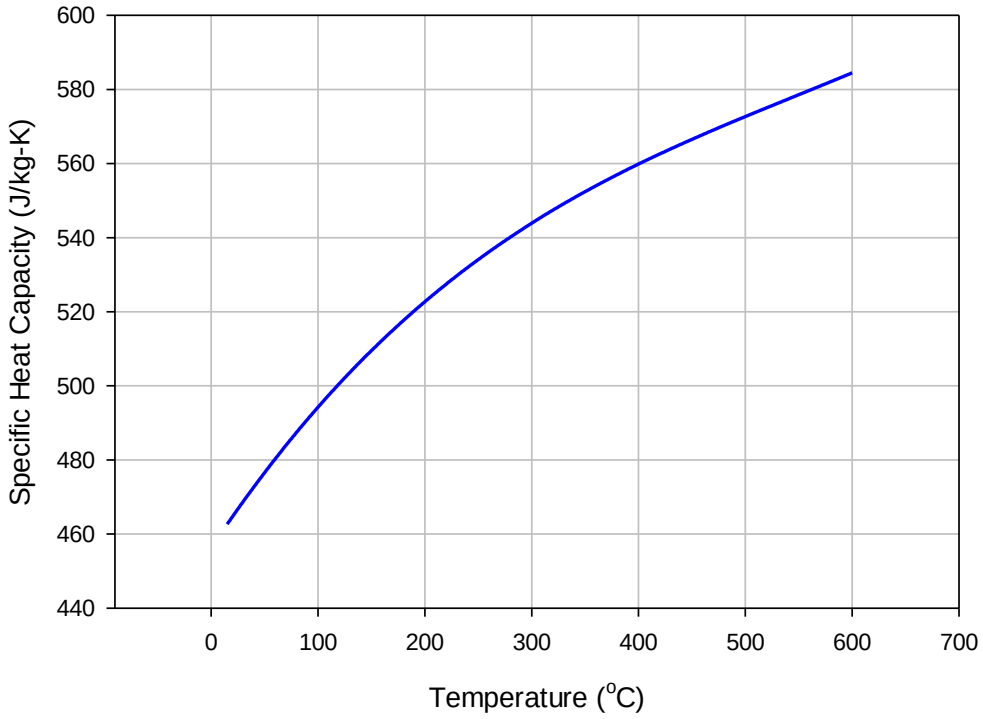

Figure 3-5
Specific heat capacity versus temperature for Type 300 series stainless steel

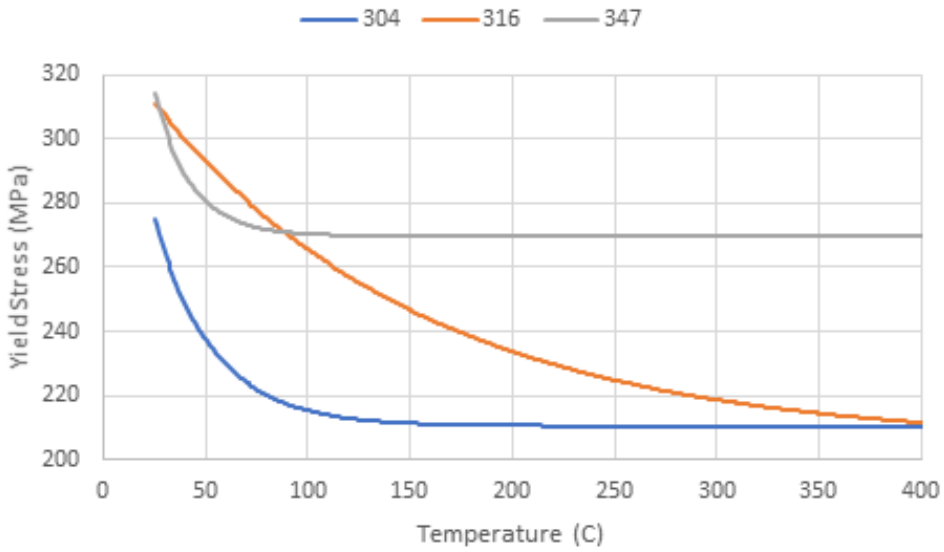

Figure 3-6
Empirical yield strength model as a function of temperature for unirradiated, annealed Type 300 series stainless steel

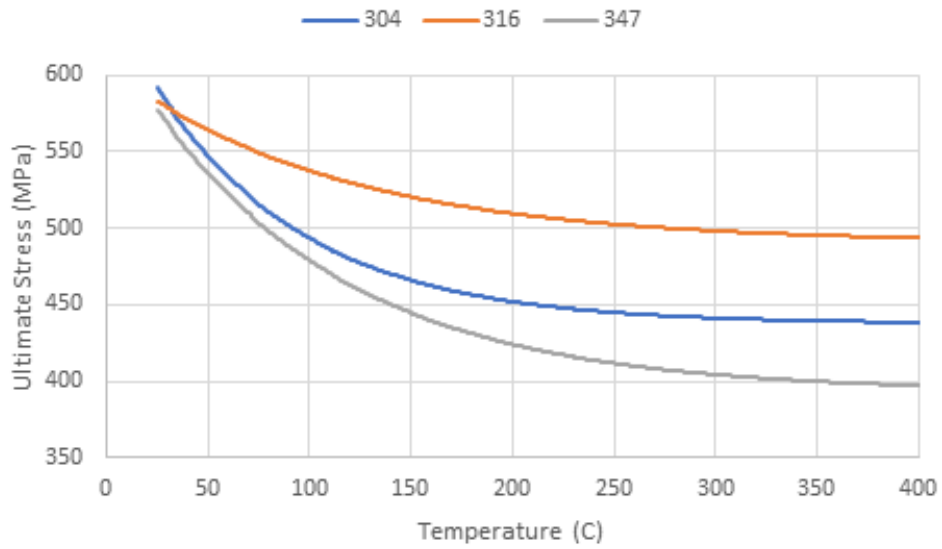

Figure 3-7
Empirical ultimate tensile strength model as a function of temperature for unirradiated, annealed Type 304, 316, and 347 series stainless steel

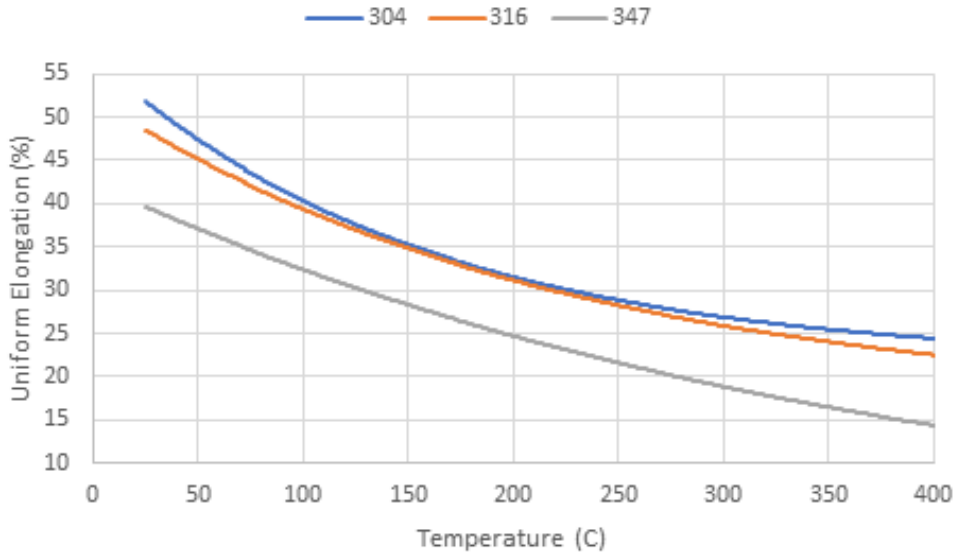

Figure 3-8
Empirical uniform elongation model as a function of temperature for unirradiated, annealed Type 304, 316, and 347 series stainless steel

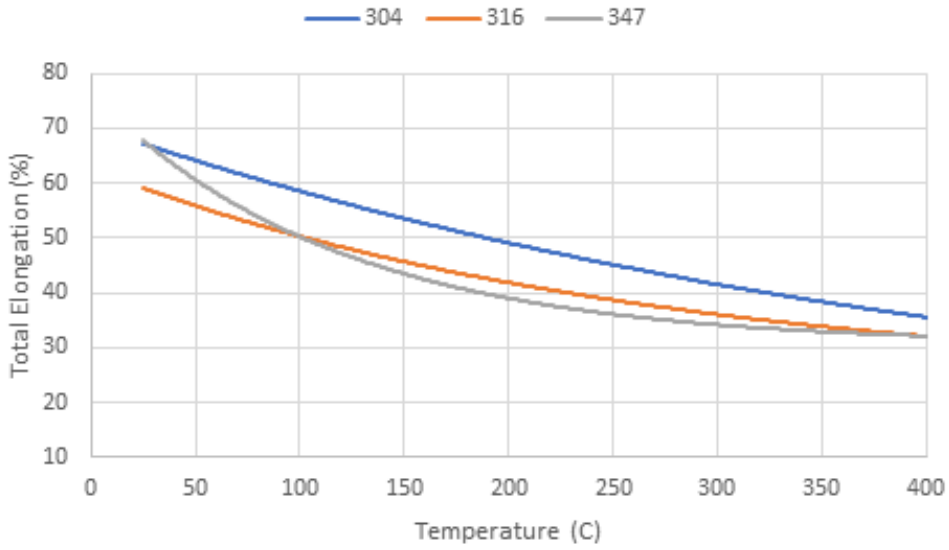

Figure 3-9
Empirical total elongation model as a function of temperature for unirradiated, annealed Type 304, 316, and 347 series stainless steel

3.5 Effects of Irradiation and Cold Work on the Mechanical Properties of 316 CW, 316 SA, and 304 SA Stainless Steel at 330°C

References on the irradiation effects on stainless steels properties [12–21] were reviewed; however, the relationships for the effects of irradiation on stainless steel used in this model were derived from data developed by the Joint Owner's Baffle Bolt (JOBB) Program [22–26] as updated in MRP-211, Revision 1 [4].

3.5.1 Modeling of Irradiation Effects at 330°C

The 0.2% yield strength, ultimate tensile strength, uniform elongation, and total elongation data for the special case of 330°C were fitted to an exponential equation, as shown in Equation 3-4a for the strength properties and Equation 3-4b for the elongation properties, with coefficients defined in Tables 3-6 through 3-9, for Types 316 CW, 316 SA, 304 SA, and 347 SA:

$$Property = A0 + A1\,[1 - \exp(-A2*d)], \text{ where d is the dose in dpa} \qquad \textbf{Eq. 3-4a}$$

for the yield and ultimate strengths, and

$$Property = A0 + A1\exp(-A2*d), \text{ where } d \text{ is the dose in dpa} \qquad \textbf{Eq. 3-4b}$$

for the uniform and total elongations.

It is noted that, in the present applications, the maximum cold work ratio is limited to 0.2, and solution-annealed material is considered to have a minimum cold work ratio of 0.01. These maximum and minimum cold work ratios are the input values for the Equation 3-4 coefficients listed in Tables 3-6 through 3-9.

Table 3-6
Materials property equations for irradiated 316 CW at 330°C

Property	Units	Property = $A_0 + A_1 (1 - \exp(-A_2 * d))$		
		A_0	A_1	A_2
0.2% yield strength	MPa	504.4221	405.6508	0.4114
Ultimate tensile strength	MPa	612.3013	356.1812	0.4158
Property	**Units**	**Property = $A_0 + A_1 * \exp(-A_2 * d)$**		
		A_0	A_1	A_2
Uniform elongation	%	0.4736	6.3729	0.4371
Total elongation	%	6.9332	8.6942	0.4203

Table 3-7
Materials property equations for irradiated 316 SA at 330°C

Property	Units	Property = $A_0 + A_1 (1 - \exp(-A_2 * d))$		
		A_0	A_1	A_2
0.2% yield strength	MPa	218.5806	570.6374	0.48
Ultimate tensile strength	MPa	479.6953	332.8633	0.3704
Property	**Units**	**Property = $A_0 + A_1 * \exp(-A_2 * d)$**		
		A_0	A_1	A_2
Uniform elongation	%	0.8529	26.6395	0.3308
Total elongation	%	8.6278	28.9933	0.336

Table 3-8
Materials property equations for irradiated 304 SA at 330°C

Property	Units	Property = $A_0 + A_1 (1 - \exp(-A_2 * d))$		
		A_0	A_1	A_2
0.2% yield strength	MPa	247.7567	545.8073	0.6219
Ultimate tensile strength	MPa	450.9427	353.3238	0.3904
Property	**Units**	**Property = $A_0 + A_1 * \exp(-A_2 * d)$**		
		A_0	A_1	A_2
Uniform elongation	%	0.4864	24.6884	1.8194
Total elongation	%	9.1247	29.9201	0.5639

Table 3-9
Materials property equations for irradiated 347 SA at 330°C

Property	Units	Property = $A_0 + A_1 (1 - \exp(-A_2 * d))$		
		A_0	A_1	A_2
0.2% yield strength	MPa	268.846	557.7723	0.6726
Ultimate tensile strength	MPa	432.9199	412.3785	0.5533
Property	**Units**	**Property = $A_0 + A_1 * \exp(-A_2 * d)$**		
		A_0	A_1	A_2
Uniform elongation	%	1.6238	18.0137	3.2398
Total elongation	%	7.3534	25.9732	0.7079

3.5.2 Generalization to Cold Work and Irradiation at 330°C

Equation 3-4, which applies to Type 304 SA and to a specific cold work ratio of 0.2 for Type 316 CW and 0.01 for Type 316 SA, as a function of irradiation dose at the temperature of 330°C, will now be generalized, also as a function of irradiation dose, to other values of cold work and temperature. This generalization is derived as a multiplicative expression as follows:

Property (irradiation, cold work, temperature) = *Property* (unirradiated) *
Cold-Work Factor * Irradiation Factor * Temperature Factor **Eq. 3-4**

The cold work factor is derived from manufacturer's data sheets on cold-worked stainless steels [27, 28] and the data developed in the JOBB program for irradiated 316 CW and 304 SA material [14]. Equations for yield strength, ultimate tensile strength, and total elongation as a function of cold work were developed from the manufacturer's data sheet at 20°C, scaled to fit the JOBB 316 CW and 304 SA data at 330°C, and fitted to Equation 3-5, with coefficients defined in Tables 3-10 through 3-13.

$$\eta_i(c) = f_0 + f_1[1 - exp(-c/c_1)] + f_2\, exp(-c/c_2) \qquad \textbf{Eq. 3-5}$$

where c is the cold work ratio, and the subscript i refers to any of the four properties modeled, as shown in Tables 3-10 through 3-13. The cold work ratios used for this fit were 0.2 for 316 CW, 0.01 for 304 SA, and 0.0 for unirradiated, annealed Type 300 series stainless steel.

Table 3-10
Cold work factors for 316 stainless steels

Property	Cold Work Factor = $f_0 + f_1 (1 - \exp(-c/c_1)) + f_2 \exp(-c/c_2)$				
	f_0	f_1	c_1	f_2	c_2
0.2% yield strength	1	6.661475	0.526629904	—	—
Ultimate tensile strength minus yield strength	14.17559717	-4.08832984	0.526629904	-13.1755972	3.3
Uniform elongation	1	-0.95921518	0.145169378	—	—
Total elongation minus uniform elongation	-2.40830696	2.857596634	0.145169378	3.408306964	0.151016372

Note: c = cold work ratio (varies from 0 to 0.2)

Table 3-11
Cold work factors for 304 stainless steels

Property	Cold Work Factor = $f_0 + f_1 (1 - \exp(-c/c_1)) + f_2 \exp(-c/c_2)$				
	f_0	f_1	c_1	f_2	c_2
0.2% yield strength	1.1485	4.964765761	0.526629904	—	—
Ultimate tensile strength minus yield strength	11.80728015	-3.26897626	0.526629904	-10.9743501	3.3
Uniform elongation	1.2105	-1.20013434	0.145169378	—	—
Total elongation minus uniform elongation	-0.98861001	1.143317172	0.145169378	1.399110009	0.151016372

Note: c = cold work ratio (varies from 0 to 0.2)

Table 3-12
Irradiation factors for 316 stainless steels

Property	Irradiation Factor = $g_0 + g_1 (1-\exp(-d/d_1)) + g_2 \exp(-d/d_2)$				
	g_0	g_1	d_1	g_2	d_2
0.2% yield strength	1.1092	1.3150	4.249894	—	—
Ultimate tensile strength minus yield strength	0.180207212	-0.11173615	6.9	0.819792788	2.3
Uniform elongation	1	-0.97	2	—	—
Total elongation minus uniform elongation	2.212499795	-1.37499964	5	-1.21249979	2

Note: Neutron dose (d) in dpa

Table 3-13
Irradiation factors for 304 stainless steels

Property	Irradiation Factor = $g_0 + g_1 (1-\exp(-d/d_1)) + g_2 \exp(-d/d_2)$				
	g_0	g_1	d_1	g_2	d_2
0.2% yield strength	1.1323	0.0478	2.11954	—	—
Ultimate tensile strength minus yield strength	0.004831455	-0.00207975	6.9	0.995168545	2.3
Uniform elongation	1.0	-0.9875	1.0	—	—
Total elongation minus uniform elongation	8.9	-7.4	2.5	-7.9	1.0

Note: Neutron dose (d) in dpa

The irradiation factor is derived directly from the irradiated material properties and is shown in Equation 3-6, with the coefficients defined in Tables 3-12 and 3-13.

$$\xi_i(d) = g_0 + g_1[1 - exp(-d/d_1)] + g_2\, exp(-d/d_2) \quad \textbf{Eq. 3-6}$$

where *d* is the dose in dpa, and the subscript *i* refers to the ith property as before. The temperature factor is derived using equations from Table 3-3 through 3-5 as follows:

$$\phi(T) = (C_0 + C_1\, e^{-C_2 T})/(C_0 + C_1\, e^{-C_2 * 330}) \text{ for } 20°C \le T \le 600° \quad \textbf{Eq. 3-7}$$

3.5.3 Generalization of Mechanical Properties to Variable Temperature, Cold Work, and Irradiation

The fundamental mechanical properties that govern material behavior are as follows:

- The elastic modulus *E*
- The yield stress at the elastic limit
- The ultimate tensile strength (the peak point on the engineering stress-strain curve)
- The uniform elongation
- The total elongation

These are generalized for variable temperature, irradiation dose, and cold work through the following set of equations.

The temperature multiplier on the yield strength and the ultimate tensile strength is kept the same as expressed in Equations 3-7 and 3-8, which were re-derived from Equation 3-3 and Tables 3-3 through 3-5. These expressions are restated below for continuity.

$$\varphi(T) = (C_0 + C_1\, e^{-C_2 T})/(C_0 + C_1\, e^{-C_2 * 330}) \text{ , } 20°C \le T \le 600°C \quad \textbf{Eq. 3-8}$$

$$YS(r_{cw}, d, T) = YS(r_{cw}, d)\ \varphi(T) \quad \textbf{Eq. 3-9}$$

$$UTS(r_{cw}, d, T) = UTS(r_{cw}, d)\ \varphi(T) \quad \textbf{Eq. 3-10}$$

where:

$$\boldsymbol{YS(r_{CW}, d)} \;=\; \boldsymbol{YSU(r_{CW}) + \{YSI - YSU(r_{CW})\}\{1 - exp(-d/d_0)\}} \qquad \textbf{Eq. 3-11}$$

$$\boldsymbol{UTS(r_{CW}, d)} \;=\; \boldsymbol{UTSU(r_{CW}) + \{UTSI - UTSU(r_{CW})\}\{1 - exp(-d/d_0)\}} \qquad \textbf{Eq. 3-12}$$

Such that

$$\boldsymbol{YSU(r_{cw}) = YSU_0 + 2(YSI - YSU_0)\, r_{cw} - (YSI - YSU_0)\, r_{cw}^2,} \qquad \textbf{Eq. 3-13}$$

and

$$\boldsymbol{UTSU(r_{cw}) = UTSU_0 + 2(UTSI - UTSU_0)\, r_{cw} - (UTSI - UTSU_0)\, r_{cw}^2} \qquad \textbf{Eq. 3-14}$$

The parameter pairs (*YSI*, *UTSI*) and (YSU_0, $UTSU_0$), which appear in Equations 3-11 through 3-14, are, respectively, the fully irradiation-saturated values of yield strength and ultimate tensile strength, and the unirradiated yield strength and ultimate tensile strength, all at 330°C; they are specially derived quantities and are defined in Table 3-14.

Table 3-14
Values for 304 and 316 stainless steel unirradiated and irradiated yield strength and ultimate tensile strength at 330°C

	YSU_0 (MPa)	YSI (MPa)	$UTSU_0$ (MPa)	UTSI (MPa)
304 SA r_{cw}=0	247.7	793.5	450.9	804.2
316 SA r_{cw}=0	218.5	789.2	479.7	812.5
316 CW r_{cw}=0.2	504.4	910.0	612.3	968.4
347 SA r_{cw}=0	268.8	826.6	432.9	845.3

It remains to define the elongation properties (uniform and total), stated earlier in Equation 3-3, for the effects of cold work and irradiation. The total elongation $\varepsilon_{TE}^{'}$ for any temperature, irradiation dose, or work hardening ratio is defined as follows:

$$\boldsymbol{\varepsilon_{TE}^{'} = \varepsilon_{UE}^{'} + \Delta\varepsilon_{TE-UE}^{'}} \qquad \textbf{Eq. 3-15}$$

$$\boldsymbol{\varepsilon'_{\mathrm{UE}} = \varepsilon_{\mathrm{UE}}(T)\, \eta_3(c)\, \xi_3(d)} \qquad \textbf{Eq. 3-16}$$

$$\boldsymbol{\Delta\varepsilon_{TE-UE}^{'} = \; [\varepsilon_{TE}(T) - \varepsilon_{UE}\,(T)]\; \eta_4(c)\; \xi_4(d)} \qquad \textbf{Eq. 3-17}$$

$\varepsilon_{\mathrm{UE}}(T)$ = (uniform elongation, function of temperature according to Tables 3-3 through 3-9)/100

$\varepsilon_{\mathrm{TE}}(T)$ = (total elongation, function of temperature according to Tables 3-3 through 3-9)/100

$\xi_i(d)$ = irradiation factor for the i[th] material property, defined in Equation 3-6, restated:

$$\boldsymbol{\xi_i(d) = g_0 + g_1[1 - \exp(-\mathrm{d}/\mathrm{d}_1)] + g_2 \exp(-\mathrm{d}/\mathrm{d}_2)} \qquad \textbf{Eq. 3-18}$$

$\eta_i(c)$ = cold-work factor for the i[th] material property, defined in Equation 3-5, restated:

$$\boldsymbol{\eta_i(c) = f_0 + f_1[1 - exp(-c/c_1)] + f_2\, exp(-c/c_2)} \qquad \textbf{Eq. 3-19}$$

c = cold-work ratio r_{cw}

d = neutron dose in dpa

The coefficients in the preceding equations are defined in Tables 3-15 and 3-16 for the cold work factors and in Tables 3-17 and 3-18 for the irradiation factors.

Table 3-15
Cold work factors for 316 stainless steels

Property	Cold Work Factor = f0 + f1 (1 - exp(-c/c1)) + f2 exp(-c/c2)				
	f_0	f_1	c_1	f_2	c_2
Uniform elongation	1.0	-0.95921518	0.145169378	—	—
Total elongation minus uniform elongation	-2.40830696	2.857596634	0.145169378	3.408306964	0.151016372

Note: c = cold work ratio (varies from 0 to 0.2)

Table 3-16
Cold work factors for 304 stainless steels

Property	Cold Work Factor = $f_0 + f_1 (1 - \exp(-c/c_1)) + f_2 \exp(-c/c_2)$				
	f_0	f_1	c_1	f_2	c_2
Uniform elongation	1.2105	-1.20013434	0.145169378	—	—
Total elongation minus uniform elongation	-0.98861001	1.143317172	0.145169378	1.399110009	0.151016372

Note: c = cold work ratio (varies from 0 to 0.2)

Table 3-17
Irradiation factors for 316 stainless steels

Property	Irradiation Factor = $g_0 + g_1 (1-\exp(-d/d_1)) + g_2 \exp(-d/d_2)$				
	g_0	g_1	d_1	g_2	d_2
Uniform elongation	1.0	-0.97	2.0	—	—
Total elongation minus uniform elongation	2.212499795	-1.37499964	5.0	-1.21249979	2.0

Note: neutron dose (*d*) in dpa

Table 3-18
Irradiation factors for 304 stainless steels

Property	Irradiation Factor = $g_0 + g_1 (1-\exp(-d/d_1)) + g_2 \exp(-d/d_2)$				
	g_0	g_1	d_1	g_2	d_2
Uniform elongation	1.0	-0.9875	1.0	—	—
Total elongation minus uniform elongation	8.9	-7.4	2.5	-7.9	1.0

Note: neutron dose (*d*) in dpa

The mathematical expressions for the yield and ultimate tensile strengths, unirradiated and irradiated, are shown as a function of temperature in Figures 3-10 and 3-11 for 304 SA and 316 CW stainless steels, respectively.

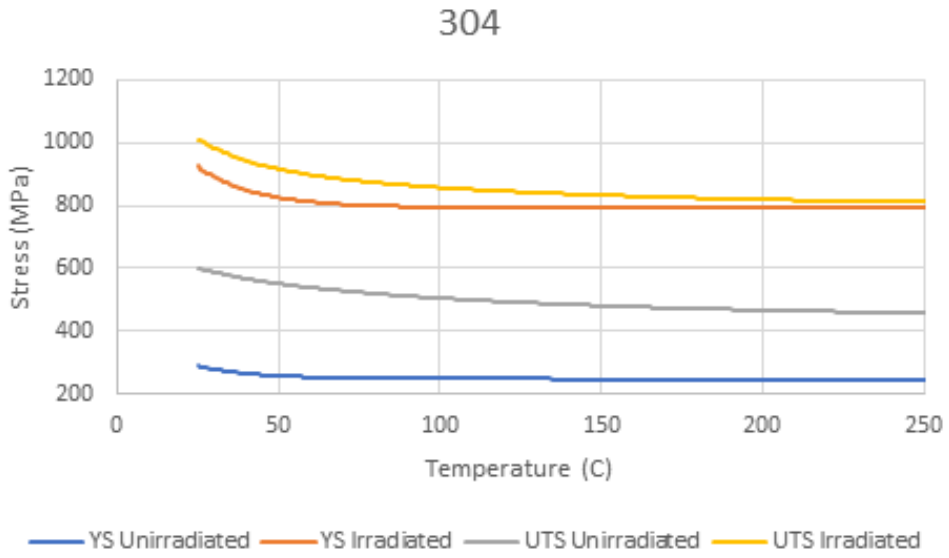

Figure 3-10
304 SA stainless steel unirradiated and irradiation-saturated yield and ultimate tensile strengths

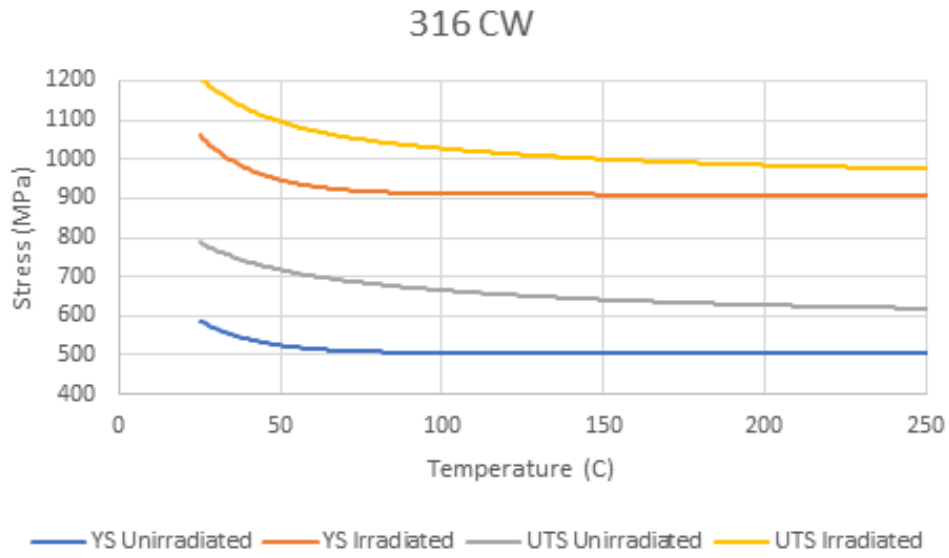

Figure 3-11
316 CW stainless steel unirradiated and irradiation-saturated yield and ultimate tensile strengths

Figures 3-12 through 3-17 show the yield and ultimate tensile strengths for types 304, 316, and 347 stainless steels at the special temperature of 330°C, which is the most relevant temperature in engineering evaluation and assessment. Figures 3-18 through 3-23 show the same properties at the room temperature of 20°C. Figures 3-24 and 3-25 show the elongation properties (uniform

and total) for the two materials 304 SA and 316 CW. It should be noted, however, that although Figures 3-12 through 3-23 show, for general interest, the properties for various cold work ratios, the applicable cold work ratios in the present work are those that characterize 316 CW, 304 SA, and 347 SA—that is, 0.2 for the former and 0.01 for the latter.

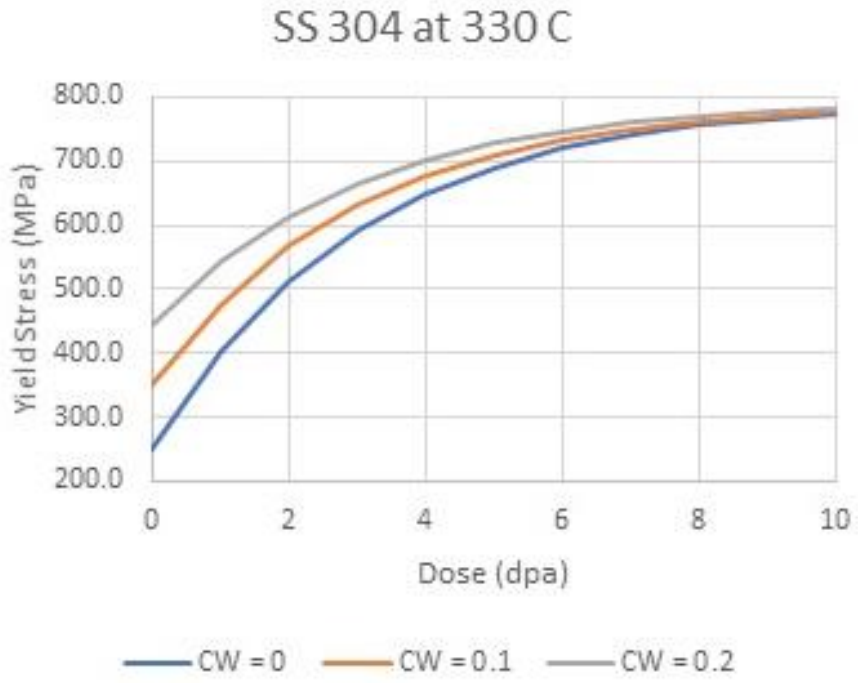

Figure 3-12
Type 304 yield stress versus dose at 330°C for $0 \leq r_{cw} \leq 0.2$

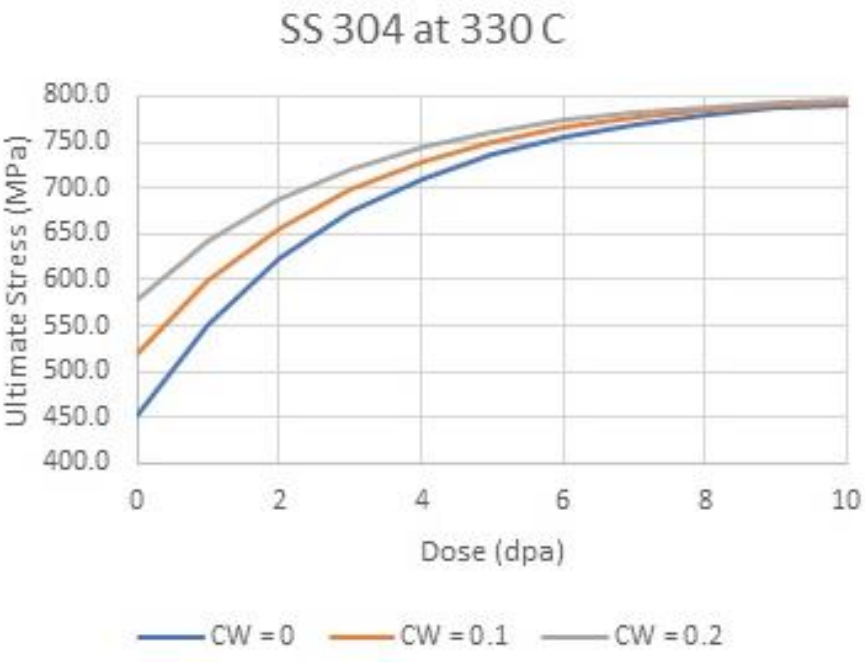

Figure 3-13
Type 304 ultimate tensile strength versus dose at 330°C for $0 \leq r_{cw} \leq 0.2$

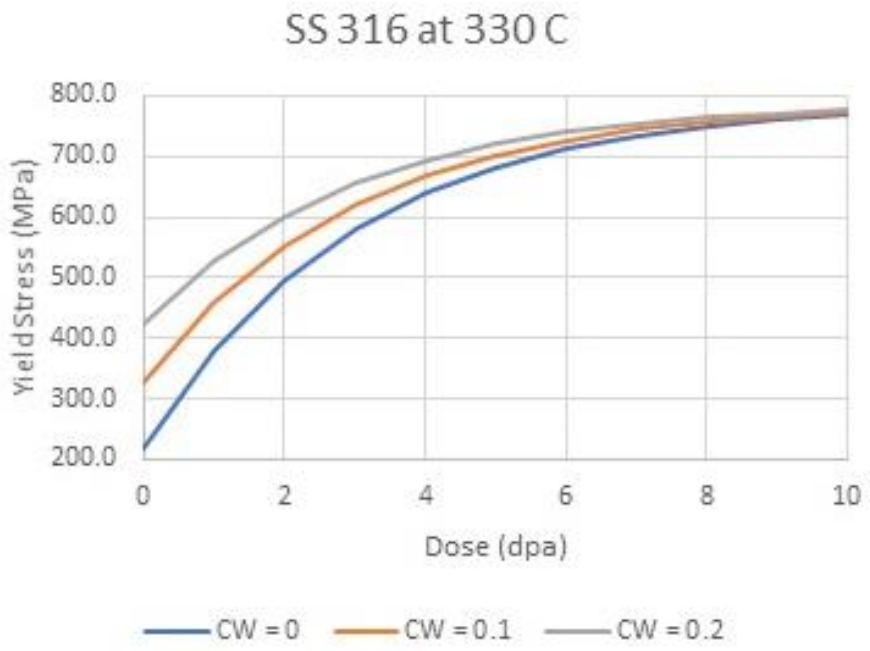

Figure 3-14
Type 316 yield stress versus dose at 330°C for $0 \leq r_{cw} \leq 0.2$

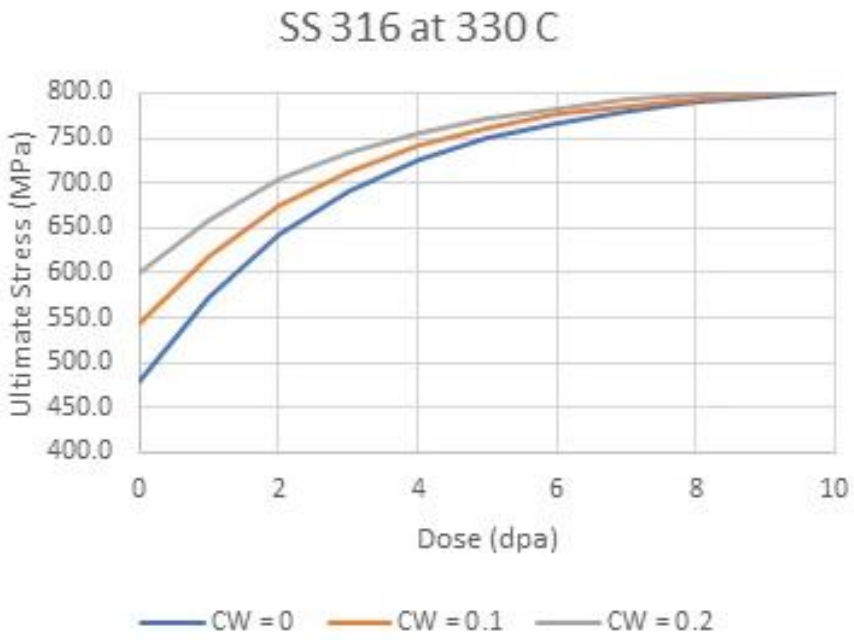

Figure 3-15
Type 316 ultimate tensile strength versus dose at 330°C for $0 \leq r_{cw} \leq 0.2$

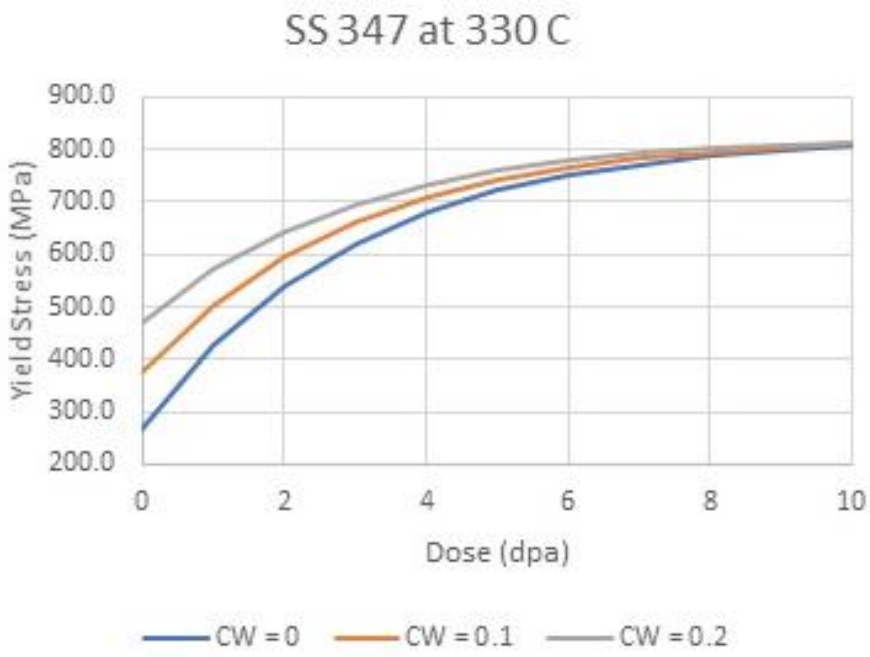

Figure 3-16
Type 347 yield stress versus dose at 330°C for 0 ≤ r_{cw} ≤ 0.2

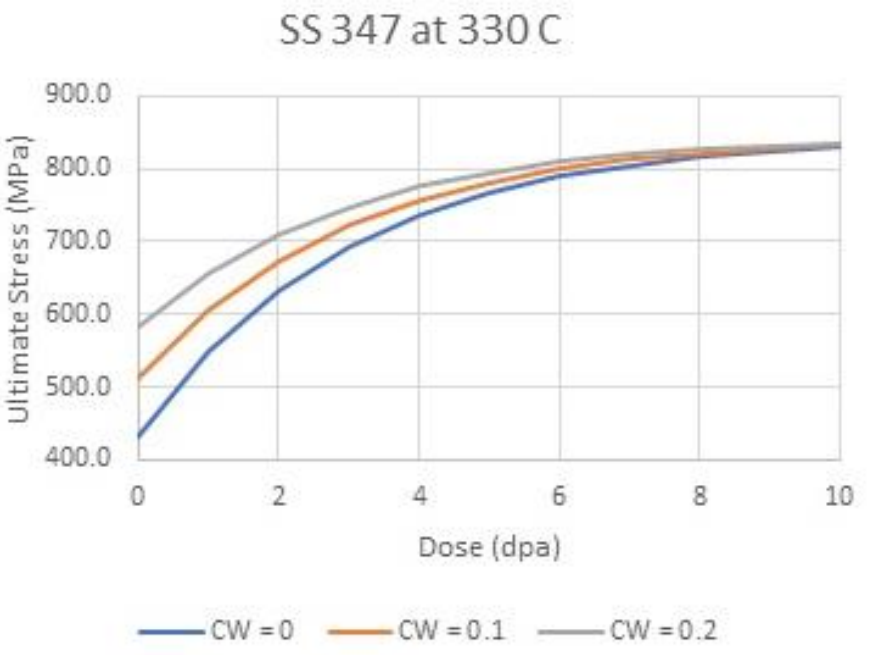

Figure 3-17
Type 347 ultimate tensile strength versus dose at 330°C for 0 ≤ r_{cw} ≤ 0.2

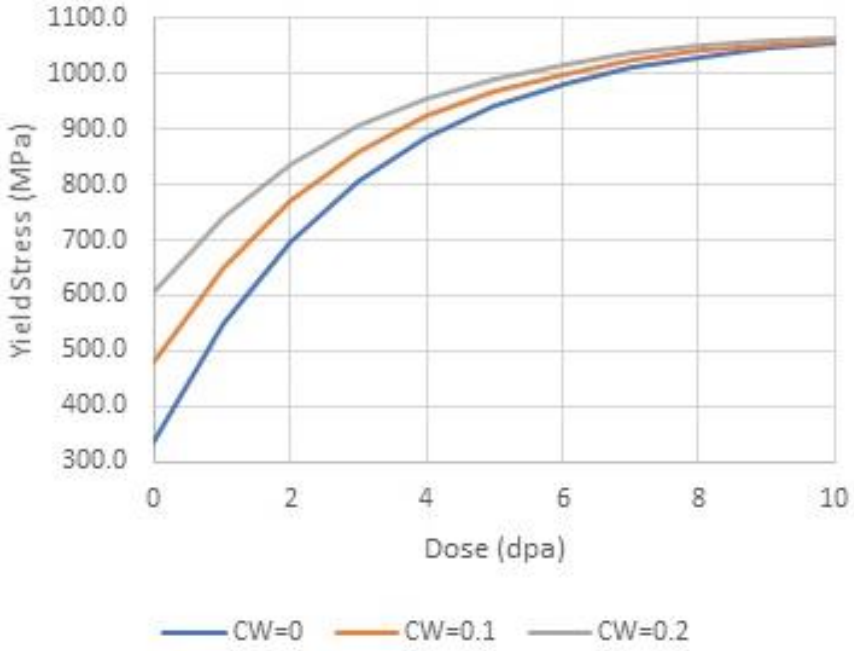

Figure 3-18
Type 304 yield stress versus dose at 20°C for $0 \leq r_{cw} \leq 0.2$

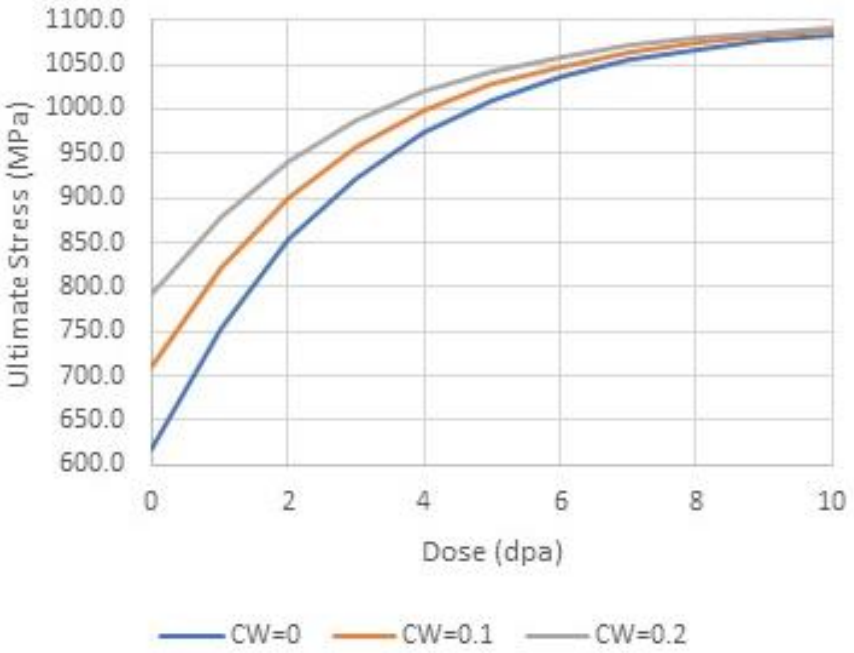

Figure 3-19
Type 304 ultimate tensile strength versus dose at 20°C for $0 \leq r_{cw} \leq 0.2$

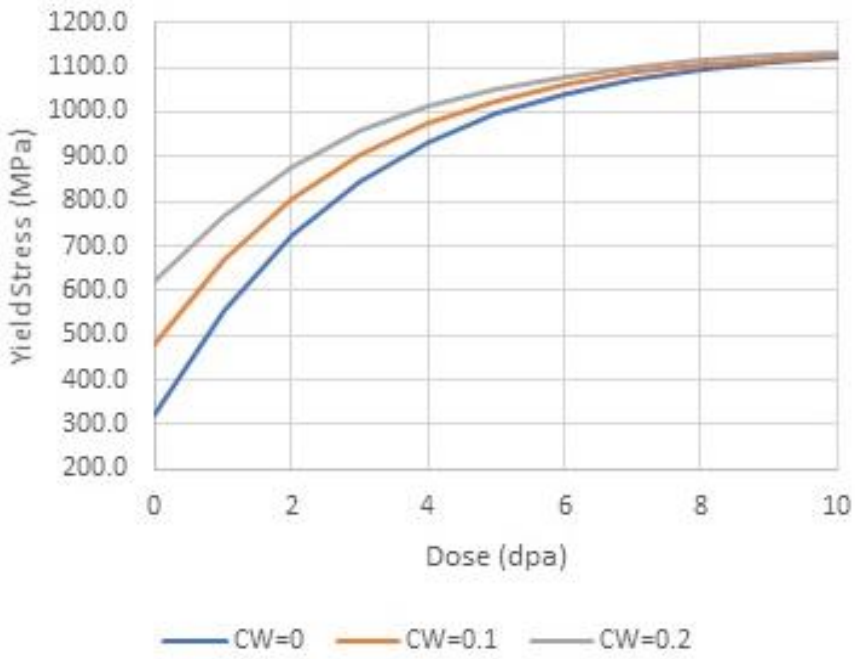

Figure 3-20
Type 316 yield stress versus dose at 20°C for $0 \leq r_{cw} \leq 0.2$

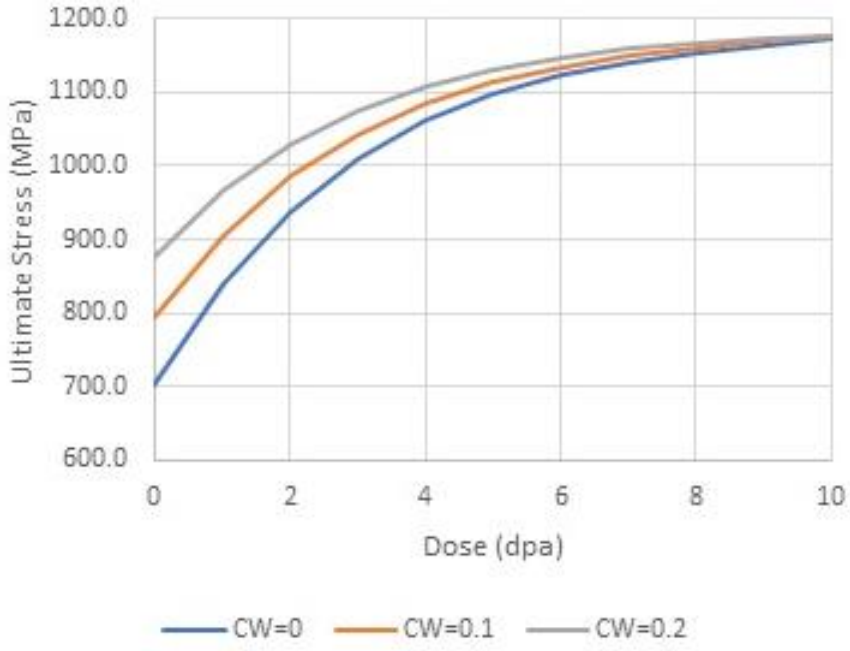

Figure 3-21
Type 316 ultimate tensile strength versus dose at 20°C for $0 \leq r_{cw} \leq 0.2$

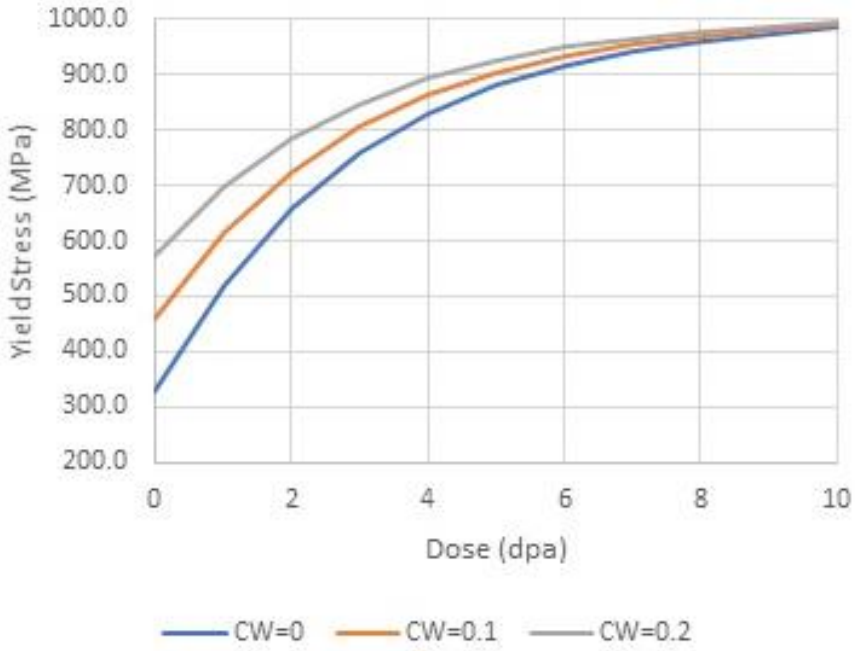

Figure 3-22
Type 347 yield stress versus dose at 20°C for $0 \leq r_{cw} \leq 0.2$

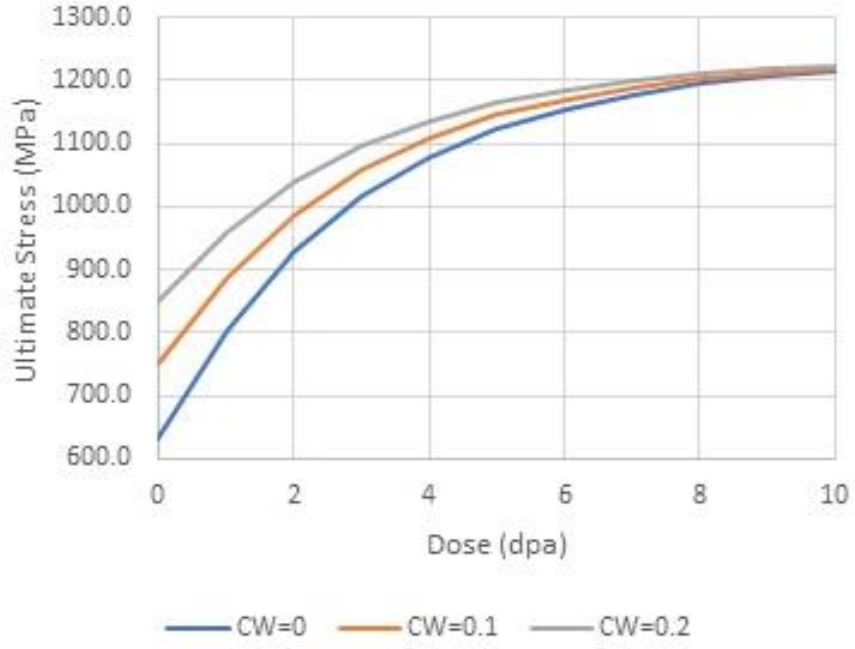

Figure 3-23
Type 347 ultimate tensile strength versus dose at 20°C for $0 \leq r_{cw} \leq 0.2$

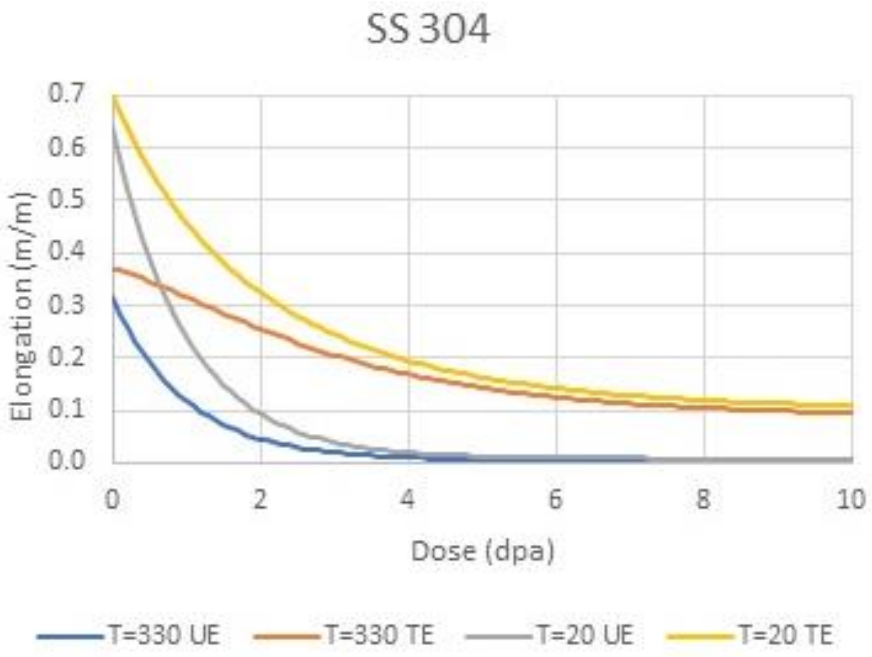

Figure 3-24
Type 304 SA uniform and total elongation versus dose at 20°C and 330°C

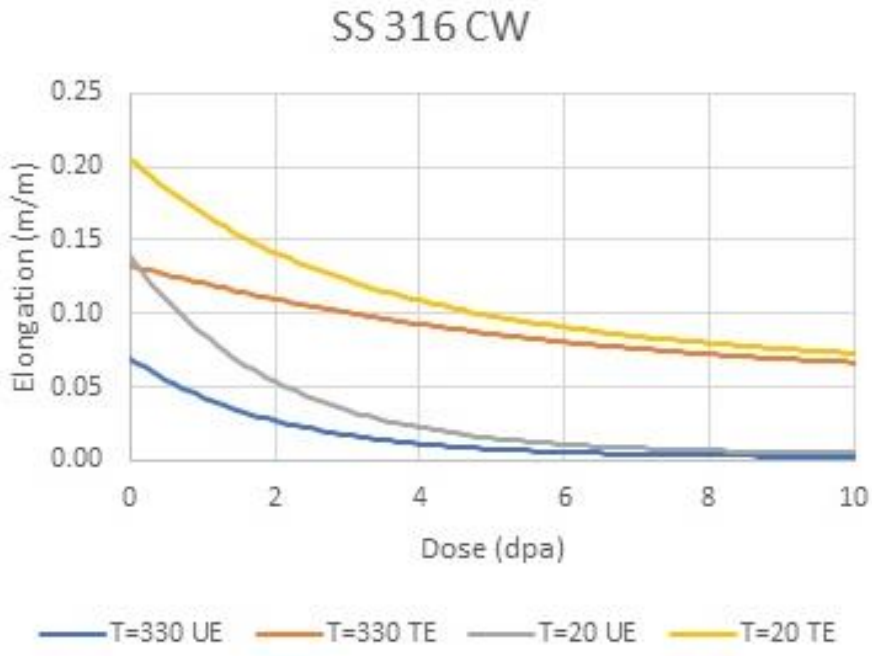

Figure 3-25
Type 316 CW uniform and total elongation versus dose at 20°C and 330°C

3.6 Generalized Uniaxial Stress-Strain Relationship

The mechanical properties described in Section 3.5 are used in defining a general form for the uniaxial stress-strain relationship. In the elastic regime, this relationship is simply $\sigma = E\varepsilon$, where E is the elastic modulus and ε is the strain. The stress-strain equation in the plastic regime for cold-worked irradiated stainless steel can now be defined as follows:

$$\boldsymbol{\sigma = \{\sigma_Y' + \Delta\sigma_{U-Ye}' [1 - exp(-(\varepsilon - \sigma_Y'/E)/\varepsilon_o')]\}, \sigma > \sigma_Y'} \qquad \textbf{Eq. 3-20}$$

Implicitly included in Equation 3-20 are the fundamental mechanical properties, described in Section 3.5 as functions of temperature, irradiation dose, and cold work. These are the elastic modulus E, the 0.2% offset yield strength, the yield stress at the elastic limit, the ultimate tensile strength, the uniform elongation, and the total elongation. Equation 3-20 is of the same form as described earlier in Equation 3-1. The pair of variables (σ, ε) defines the stress and strain coordinates on the stress-strain curve. The sequence of calculations for Equation 3-20 is as follows:

1. Determine the 0.2% offset yield strength from Equation 3-9 as follows:

   $\sigma_{0.002}^{'} = YS(r_{cw}, d)\ \varphi(T)$

2. Calculate the quantity using Equations 3-9 and 3-10, as follows:

   $\Delta\sigma_{U-Y}' = UTS(r_{cw}, d)\ \varphi(T) - YS(r_{cw}, d)\ \varphi(T)$

3. Calculate the quantity:

   $\Delta\sigma_{U-Ye}' = \Delta\sigma_{U-Y}'\ /\ exp(-0.002/\varepsilon_0);\ \ \varepsilon_o = \ 0.2486829$

4. Calculate the ultimate strength point on the curve:

   $\sigma_U' = \sigma_{0.002}^{'} + \Delta\sigma_{U-Y}^{'}$

5. Calculate the yield stress at the elastic limit point on the curve:

   $\sigma_Y' = \sigma_U^{'} - \Delta\sigma_{U-Ye}^{'}$

6. Calculate:

   $\varepsilon_o' = \varepsilon_o\ \varepsilon_{\mathrm{UE}}^{'}$,

   where $\varepsilon_{\mathrm{UE}}^{'}$ is defined in Equation 3-16.

7. Substituting the previously calculated quantities into Equation 3-20, together with the desired value of strain ε, determines the corresponding stress level $\sigma > \sigma_Y^{'}$.

3.6.1 Stress-Strain Curves

Figures 3-26 through 3-29 show the stress-strain curves for the two materials. Figures 3-26 through 3-29 show the stress-strain curve for unirradiated stainless steel Types 304, 316, and 347, respectively, as a function of temperature and cold work. Figures 3-28 and 3-29 show the stress-strain curve for 304 SA and 316 CW, respectively, as a function of temperature and dose.

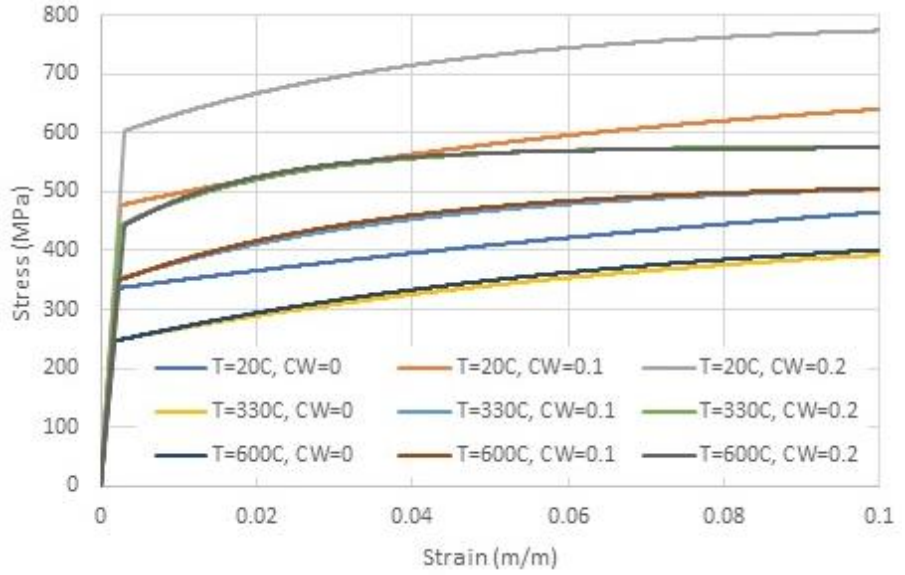

Figure 3-26
Unirradiated Type 304 stress-strain curve as a function of temperature and cold work

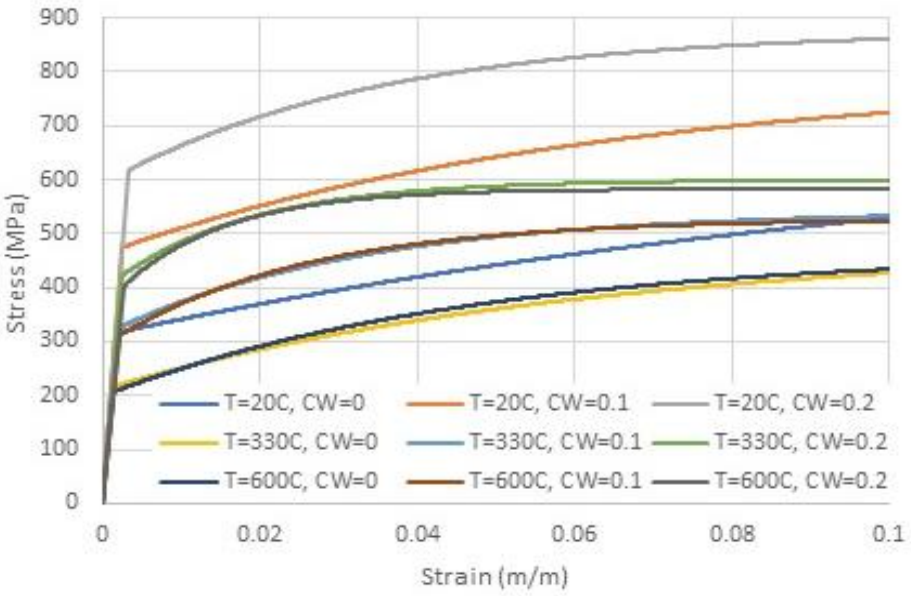

Figure 3-27
Unirradiated Type 316 stress-strain curve as a function of temperature and cold work

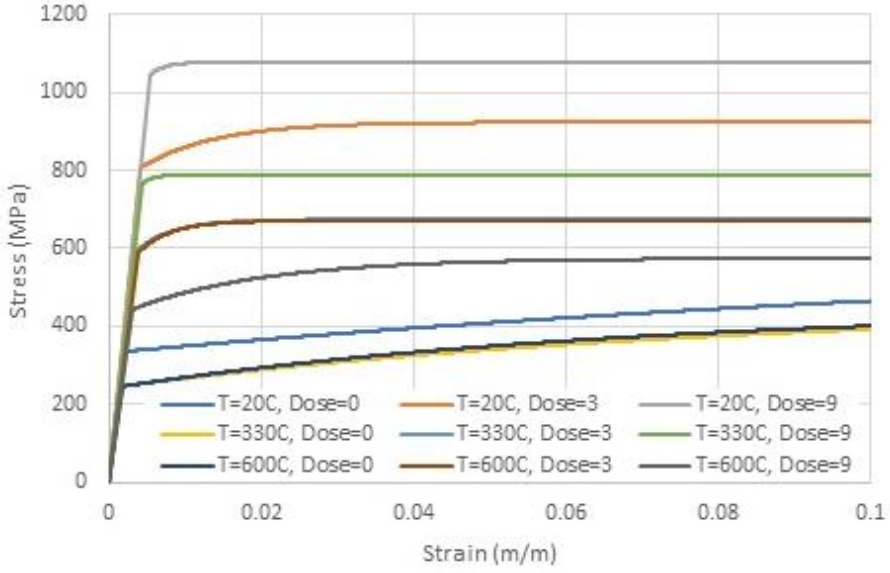

Figure 3-28
Type 304 SA stress-strain curve as a function of temperature and dose in dpa

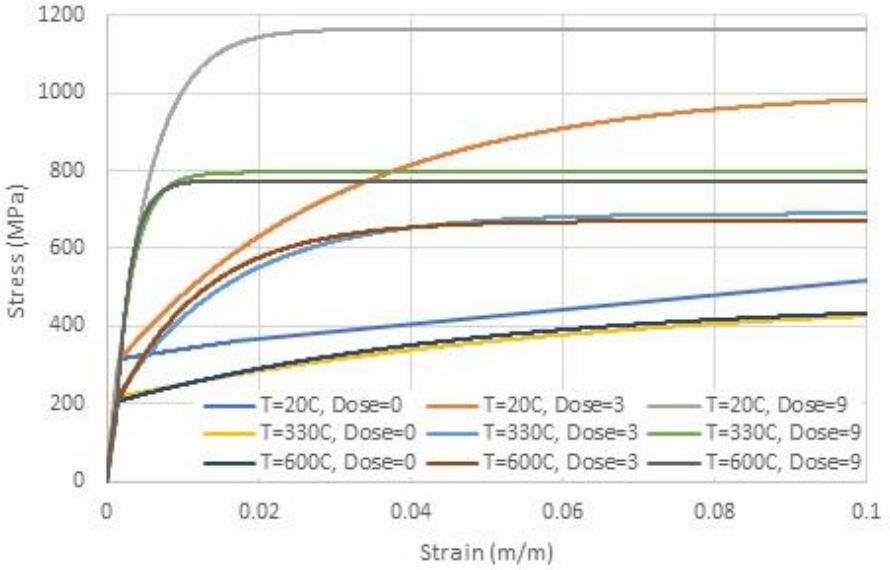

Figure 3-29
Type 316 CW = 0.2 stress-strain curve as a function of temperature and dose in dpa

3.7 Calculation of Thermal Expansion Strain

Three methods are used to calculate thermal expansion based on two sources of data—the *ITER Material Properties Handbook* [12] and the 2001 ASME Boiler & Pressure Vessel Code, Section II, Part D, Table TE-1, Page 651 [13]. All three methods should give equivalent results; the difference between them is due to the manner in which the thermal expansion data were depicted, as will become clear from the derived expressions. The three methods are implemented in IRADSS as user options, as shown below:

- **Option 1:** the use of the secant coefficient of thermal expansion, $\alpha_{se}(T)$, based on the ITER thermal expansion data, from which the expression for $\alpha_{se}(T)$ is derived, limited to a stress-free reference temperature T_{REF} of 20°C
- **Option 2:** the direct use of thermal expansion strain data in the ASME Boiler & Pressure Vessel Code [13], which can be used for any stress-free reference temperature
- **Option 3:** similar to Option 2, the direct use of the ITER thermal expansion strain data that are valid for any stress-free reference temperature

The default option is Option 2, which works for any stress-free reference temperature. Option 1 is limited to T_{REF} = 20°C; any attempted use of other values of T_{REF} for this option will result in an error termination in IRADSS.

3.7.1 The ITER Secant Coefficient of Thermal Expansion—Option 1

The following equation expresses the thermal expansion strain, ε_{th} (T), as follows:

$$\boldsymbol{\varepsilon_{th}(T) = \alpha_{se}(T)\,(T - T_{REF});\ \alpha_{se}(T) = C_1 + C_2 T + C_3 T^2}$$

The coefficients C_1, C_2, and C_3 are given in Table 3-2 in the row labeled α_{se}^{ITER}, and T_{REF} = 20°C. The increment in thermal expansion from T_1 to T_2 is

$$\boldsymbol{\Delta\varepsilon_{th}(T_2, T_1) = \alpha_{se}(T_2)\,(T_2 - T_{REF}) - \alpha_{se}(T_1)\,(T_1 - T_{REF})} \qquad \textbf{Eq. 3-21}$$

3.7.2 ASME Thermal Expansion—Option 2

The incremental thermal expansion $\Delta\varepsilon^{th}$ from T_1 to T_2 is calculated as follows:

$$\boldsymbol{\Delta\varepsilon_{th}(T_2, T_1) = C_1(T_2 - T_1) + C_2\left(T_2^2 - T_1^2\right) + C_3\left(T_2^3 - T_1^3\right)} \qquad \textbf{Eq. 3-22}$$

The coefficients C_1, C_2, and C_3 are given in Table 3-2 in the row for ε_{TH}^{ASME}.

3.7.3 Direct Use of the ITER Thermal Expansion Fit—Option 3

Rather than using the secant coefficient of expansion as in Option 1, the following calculation of the increment in thermal expansion can be used with equivalent accuracy:

$$\boldsymbol{\Delta\varepsilon_{th}(T_2, T_1) = C_1(T_2 - T_1) + C_2\left(T_2^2 - T_1^2\right) + C_3\left(T_2^3 - T_1^3\right)} \qquad \textbf{Eq. 3-23}$$

The coefficients C_1, C_2, and C_3 are defined in Table 3-2 in the row labeled ε_{TH}^{ITER}.

3.7.4 Thermal Expansion Comparison

All three methods described in the preceding and implemented into IRADSS give thermal expansion values that are accurate to the limits of machine accuracy and should not depend on the time-step size for unconstrained thermal expansion. It is important to note, however, that if thermal expansion is fully or partially constrained, the accuracy of integration of the thermal stresses is step-size-dependent. The thermal expansion strain computed by the three methods is shown in Figure 3-30 for a T_{REF} of 20°C.

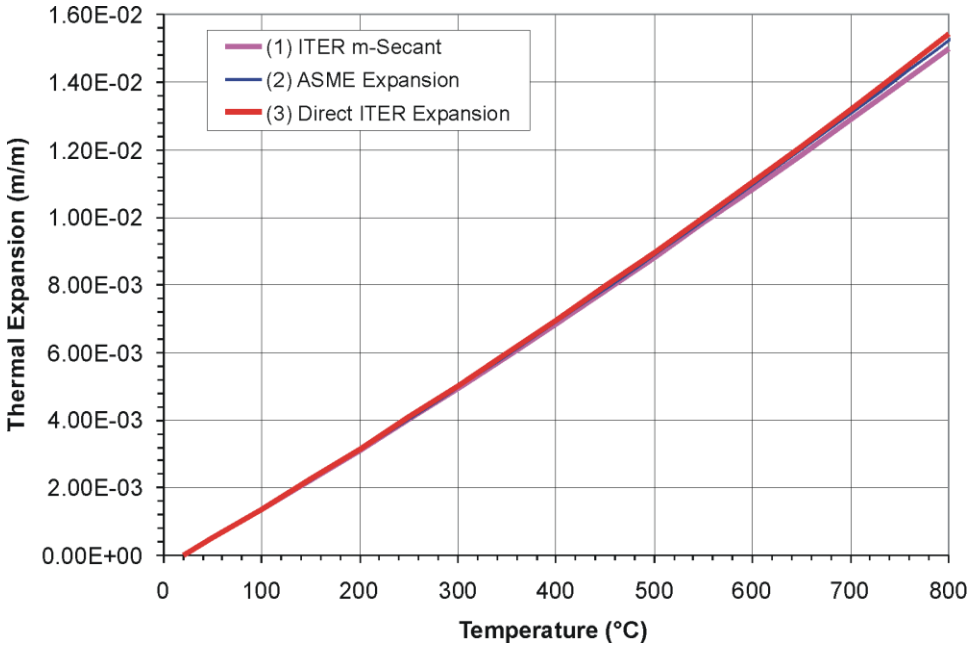

Figure 3-30
Thermal expansion computed with the three IRADSS options

3.8 Void Swelling and Irradiation Creep

Significant efforts have been undertaken to characterize the mechanisms of creep and swelling in stainless steels due to irradiation [29–36]. Two alternative models were developed for inclusion in IRADSS [5]—empirically based and models based on cluster dynamics (CD). The empirical models are based on data extracted from fast-breeder reactor experiments, where the irradiation conditions are different from those of PWRs, and their application to the stainless steels of PWR internals might introduce a degree of uncertainty in the analysis results. For example, the irradiation temperature is generally higher, and the different neutron spectrum induces a lower helium-to-damage ratio than for PWR internals. The more advanced physics-based CD models would eliminate such sources of uncertainty.

The CD-based models for both void swelling and creep were developed in the form of call-up tables generated using the EPRI PWR Internals Cluster dynamics (EPIC) code [37]. However, because the EPIC models—namely, the CD-based void swelling model and creep look-up tables—have not been fully validated, only the empirical versions of those models, described in the following, are recommended for use and are accessible by the user for any life extension analyses utilizing the IRADSS software. Because the CD-based models are not yet made available to the user, they have been excluded from this version of MRP-135 and from IRADSS.

3.8.1 Void Swelling: Empirical Model

For the empirical model, the stress-free swelling rate for 304 SA stainless steel is given by the following equation [36, 38]:

$$S'_{SA} = 2\,\varphi\,\dot{\varphi}^{-0.731}\exp[22.106 - 18558/(T + 273.15)] \qquad \textbf{Eq. 3-24}$$

where

S'_{SA} = volumetric swelling rate (%/dpa)

φ = neutron dose (dpa)

$\dot{\varphi}$ = neutron dose rate (10^{-7} dpa/sec)

T = temperature (°C)

The stress-free swelling rate for 316 CW stainless steel is given by the following equation [36]:

$$S'_{CW} = N\left[Q + 2\,\varphi\left(1 - \exp(M\,\varphi)\right)\right]\dot{\varphi}^{-0.731}\,exp\;\;[22.106 - 18558/(T + 273.15)] \qquad \textbf{Eq. 3-25}$$

where:

S'_{CW} = volumetric swelling rate (%/dpa)

N = 0.9

Q = 10.0

M = -0.010

φ = neutron dose (dpa)

$\dot{\varphi}$ = neutron dose rate (10^{-7} dpa/sec)

T = temperature (°C)

With the values shown for *N*, *Q*, and *M*, 316 CW stainless steel swells slightly more than 304 SA, up to about 10 dpa, and then shows less swelling than 304 SA due to the cold work. The maximum void swelling rate is limited to 1%/dpa [30, 35]. The data sources from which Equations 3-24 and 3-25 were derived indicate that a stress-enhanced swelling term should be included [29, 36], as shown in Equation 3-26. However, upon expert-panel evaluation, stress-enhanced swelling was judged to be unjustified and was consequently deactivated in the model, but it was retained in this report for completeness.

$$\Delta S = S'\,\Delta\varphi(1 + F\bar{\sigma}) \qquad \textbf{Eq. 3-26}$$

where

ΔS = incremental swelling (%)

S' = stress-free swelling rate given by either S'_{SA} or S'_{CW} (%/dpa)

$\Delta\varphi$ = neutron dose increment (dpa)

$\bar{\sigma}$ = von Mises effective stress (MPa)

F = 0.005 for 316 CW stainless steel (1/MPa)

The quantity ΔS enters into the constitutive derivations (see Steps 1–16 in Section 2) as

$$\Delta\varepsilon_{ij}^{V} = \Delta\varepsilon^{V_{irr}}\delta_{ij} = \Delta S\ \delta_{ij} \quad \text{Eq. 3-27}$$

The void swelling affects the temperature-dependent elastic modulus as described by the following equation [39]:

$$E(T,S) = E(T) \,/\, (1+S)^2 \quad \text{Eq. 3-28}$$

3.8.2 Irradiation Creep Empirical Model

In the original formulation of the empirical creep model, creep is assumed to begin after an incubation period, which was found to be physically unjustifiable (MRP-211, Version 1 [4]) and was changed as presented further below. However, the original model is retained in this report to maintain historical continuity. The original model is based on the synthesis irradiation creep data shown in Figure 3-31 together with linear regression [29, 31–34] fits. For this model, the vertical axis in Figure 3-31 is effective creep strain (m/m), and the horizontal axis is the product of effective stress (MPa) and dose (dpa). Both axes have been adjusted from hoop stress and hoop strain to effective stress and effective strain as shown. (Note that these tests were on pressurized closed cylinders.) For 304 (SA304L), the effective creep strain increment is $3.06\text{x}10^{-6}$ m/m per MPa per dpa increment. For 316 (CW316), the effective creep strain increment is $2.19\text{x}10^{-6}$ m/m per MPa per dpa increment following a 722 MPa-dpa threshold before creep begins. For 316 (CW316), the effective creep strain increment is $2.19\text{x}10^{-6}$ m/m per MPa per dpa increment following a 905 MPa-dpa threshold before creep begins. Note that the creep rate is not a function of temperature.

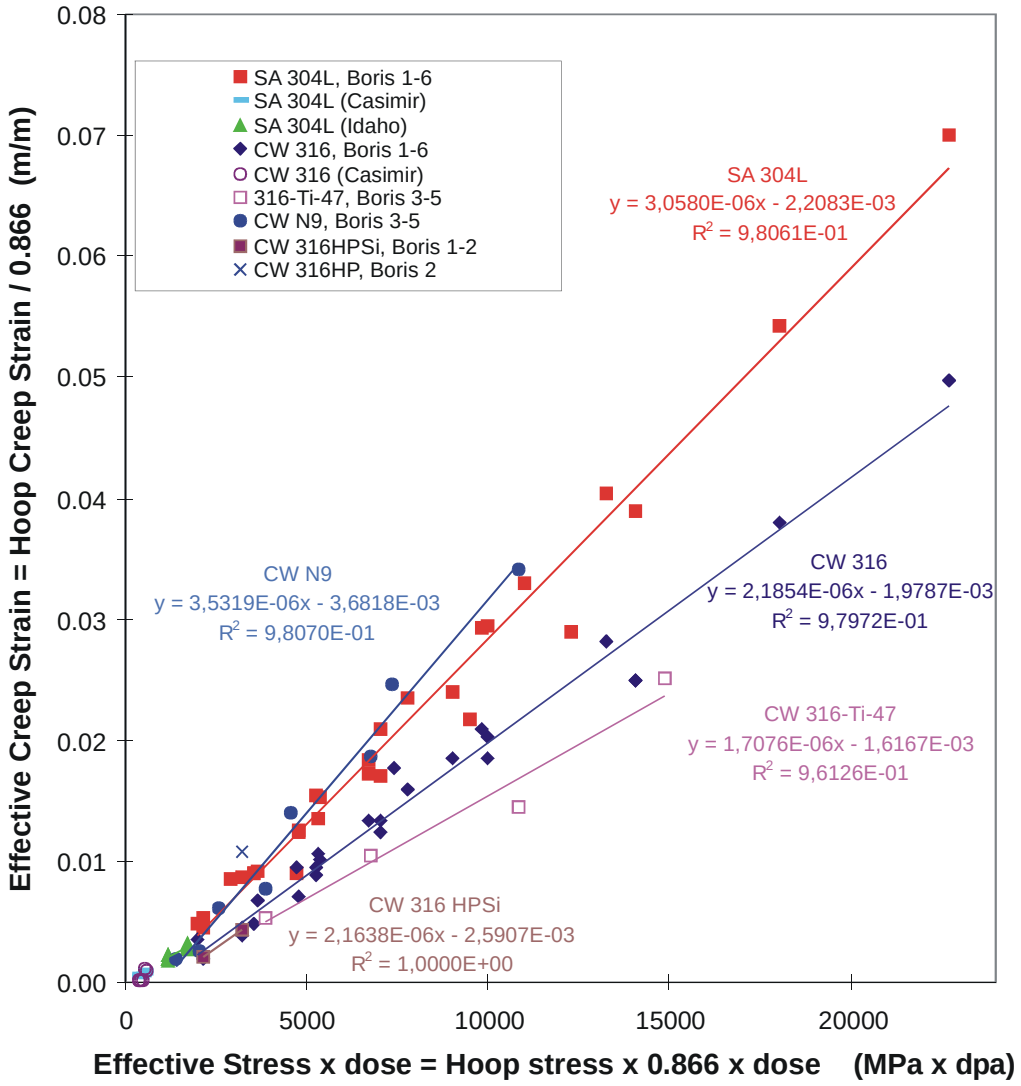

Figure 3-31
Synthesis irradiation creep data and linear regression fits

The irradiation creep rate equation used in the material model is shown in the following:

$$\bar{\varepsilon}' = \bar{\sigma} B_0 \qquad \text{Eq. 3-29}$$

where

$\bar{\varepsilon}'$ = effective creep rate (%/dpa)

$\bar{\sigma}$ = von Mises effective stress (MPa)

B_0 = creep compliance (%/MPa-dpa)

The creep compliance values for 316 CW and 304 SA are 0.0002185 %/MPa-dpa and 0.0003058 %/MPa-dpa, respectively. These values apply to temperatures in the range of 250–500°C. Typical PWR temperatures are below 400°C.

The incremental creep strain is given by

$$\Delta\bar{\varepsilon} = \bar{\varepsilon}'\dot{\varphi}\Delta t \qquad \textbf{Eq. 3-30}$$

Equation 3-30 enters into the constitutive formulation (Steps 1–16 in Section 2**)** as:

$$\Delta\varepsilon_{ij}^{C_{irr}} = \Delta\bar{\varepsilon}\ \delta_{ij} \qquad \textbf{Eq. 3-31}$$

where $\dot{\varphi}$ is the neutron dose rate in dpa/sec and Δt is the time increment in seconds.

The creep model previously described and depicted in Figure 3-31 included an incubation period for irradiation creep based on the linear regression of high irradiation dose creep data. However, the updated MRP-211, Revision 1 [4], recommends removing this incubation period because there is no clear physical mechanism to explain such an incubation period. Accordingly, Figure 3-31 is replaced by Figure 3-32, and IRADSS software was similarly updated.

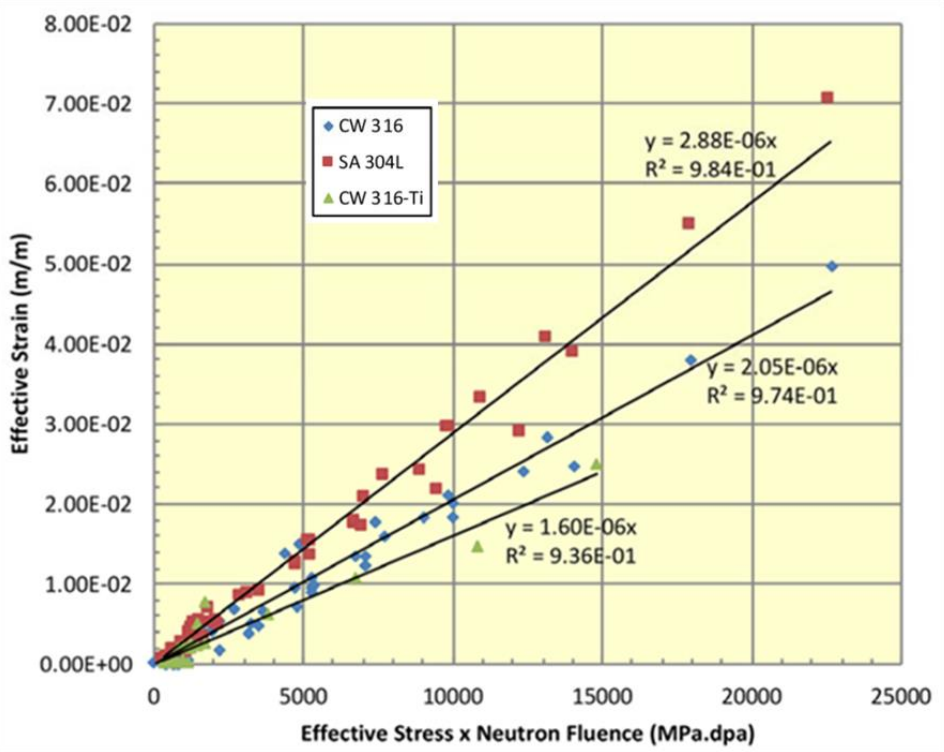

Figure 3-32
Irradiation creep data and linear regression fits: revised model (Duplicate of Figure 2-40 from MRP-211, Revision 1 [4].)

3.9 Failure Model

There are two potential causes for failure of bolted and welded connections in PWR core support structures under long-term operational conditions: IASCC and irradiation-induced loss of ductility. Material embrittlement due to excessive void swelling has been observed in stainless steel materials irradiated under unusually low dose rate at relatively high temperature [29, 34], which may be well outside PWR environments but is included here for completeness. A failure

model is formulated in which the potential for failure by any of these failure regimes is quantified in the form of a nondimensional damage index. This damage index is calculated and printed out for each failure regime separately as time-dependent state variables that represent the relative proximity to failure of the component.

3.9.1 IASCC Initiation: Empirical Model Based on MRP-211, Revision 1

The IASCC failure model development has undergone significant changes since the publication of MRP-135, Revision 1, primarily due to the availability of laboratory test data, which are summarized in MRP-211, Revision 1 [4]. An evaluation of these data indicates that the effective stress for IASCC initiation, after a threshold value of approximately $\geq 2 \times 10^{21}$ n/cm^2 (E > 1.0 MeV) or ~3 dpa, continues to decrease continuously with doses to a level of about 240 MPa (35 ksi) at 80 dpa (~5.33×10^{22} n/cm^2, E > 1.0 MeV). This necessitated a modification of the IASCC failure model. It is noted, however, that such modification can be only empirical, as depicted in Figure 3-33 as proposed in MRP-211, Revision 1 [4].

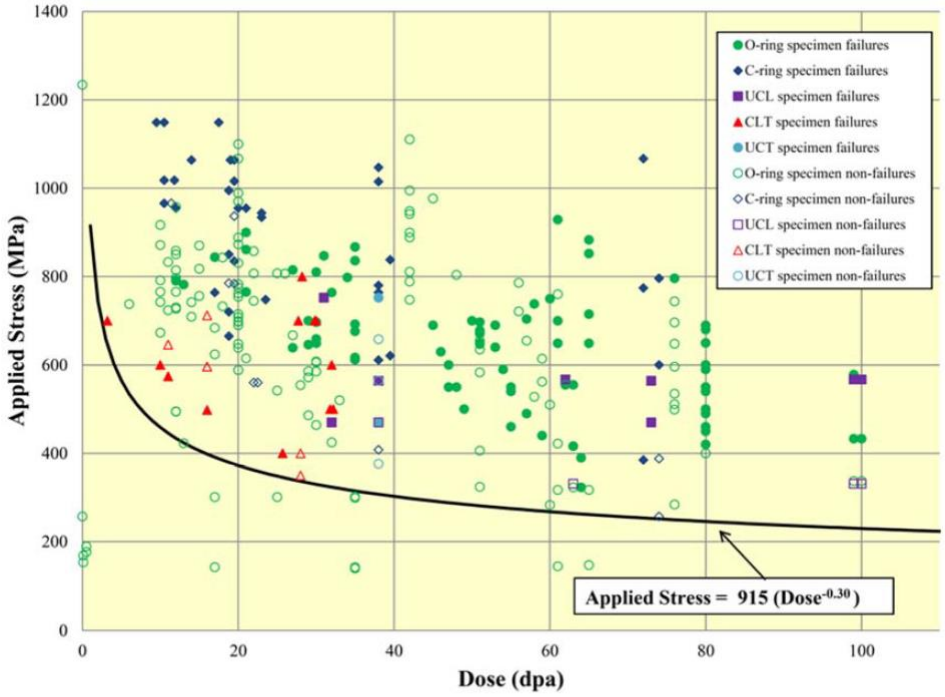

Figure 3-33
IASCC flaw initiation trend curve and model for stress as function of time (Duplicate of Figure 2-47 from MRP-211, Revision 1 [4].)

As seen in Figure 3-33, the proposed curve is the absolute lower bound of the data, which does not permit any probabilistic treatment of IASCC initiation. Furthermore, the gap in the database for this model is significant, as described in Reference [4] and summarized below:

- The available IASCC initiation data have been obtained primarily on Type 316 CW stainless steels, with limited or minimal data on SA Type 304, 304L, 316, and 347 stainless steels; cast austenitic stainless steel; stainless steel welds; and weld heat-affected zone materials.

- The data do not define an effect of temperature on IASCC initiation because most of the data have been obtained on materials irradiated below 325°C (617°F). Thus, it can only be assumed that the range of temperatures obtained in PWR internals is sufficient to initiate IASCC and that the other operating parameters (stress state and dose) are the predominant parameters to correlate to IASCC initiation.
- The database does not include potential effects of additional precipitate phases, voids, and cavities, which have been observed in stainless steels irradiated to high neutron dose levels at temperatures above 325°C (617°F). It is noted, parenthetically, that such effects are considered in the CD model for void swelling, which is not part of this revision of MRP-135.
- The IASCC initiation data, available but not considered in the Figure 3-33 model, include some testing on stainless steels irradiated in the BOR-60 fast reactor. Several studies have shown that materials irradiated in this fast reactor show lower susceptibility to IASCC than those irradiated in light water reactors.

It is further noted that the IASCC initiation model in Figure 3-33 is based on test-reactor data for specimens that by necessity do not reflect the operational history of a typical PWR's internal components. This adds another item to the data gap, namely, model validation against field data from operating reactors.

For all the aforementioned reasons, it was felt prudent to retain, in this report as well as in the IRADSS software, both models—that is, the MRP-211 model depicted in Figure 3-33 and the old MRP-Revision 1 model. The latter offers some semi-analytical features that could be useful for future model updating as the data gaps in the MRP-211 model are gradually closed and a validated IASCC initiation model is undertaken.

3.9.2 IASCC Initiation: Original Model of MRP-135, Revision 1

Under IASCC conditions, failure is assumed to occur when the component becomes susceptible to stress corrosion cracking after a certain period of irradiation. The length of time when the material becomes fully susceptible depends on the irradiation dose. The potential for stress corrosion cracking is defined by an IASCC susceptibility stress [5]. The effective stress at which IASCC susceptibility (σ_{IASCC}) initiates is defined as follows:

$$\boldsymbol{\sigma_{IASCC} = S(d)\,\sigma_y(T, d, \varepsilon^{pl}_{eff})} \qquad \textbf{Eq. 3-33}$$

In Equation 3-33, *d* is dose, and the IASCC yield stress multiplication factor, *S(d)*, is defined as shown in Figure 3-34, which relates the applied stress to the cumulative irradiation dose after which the material becomes susceptible to stress corrosion cracking. Because the yield stress is a function of dose, temperature, and effective plastic strain, the IASCC susceptibility stress depends on the loading path of a material point in the structure and, as a result, will have a different shape than the yield stress multiplication factor, *S(d)*, shown in Figure 3-34. The typical dependency of the IASCC susceptibility stress for 304 SA and 316 CW at 330°C and zero effective plastic strain is shown in Figures 3-35 and 3-36, respectively.

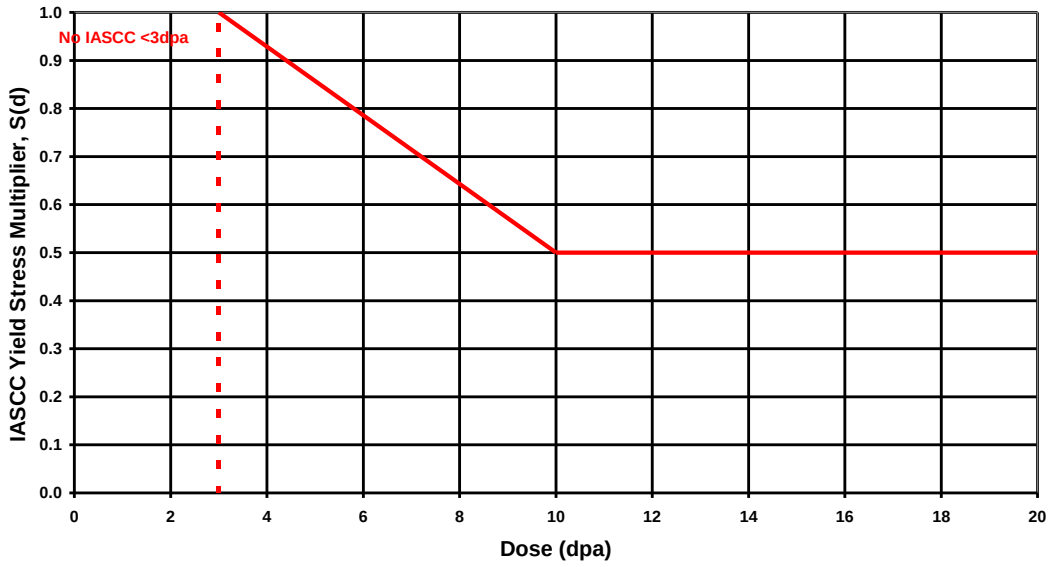

Figure 3-34
Variation of IASCC multiplication factor *S(d)* with irradiation dose

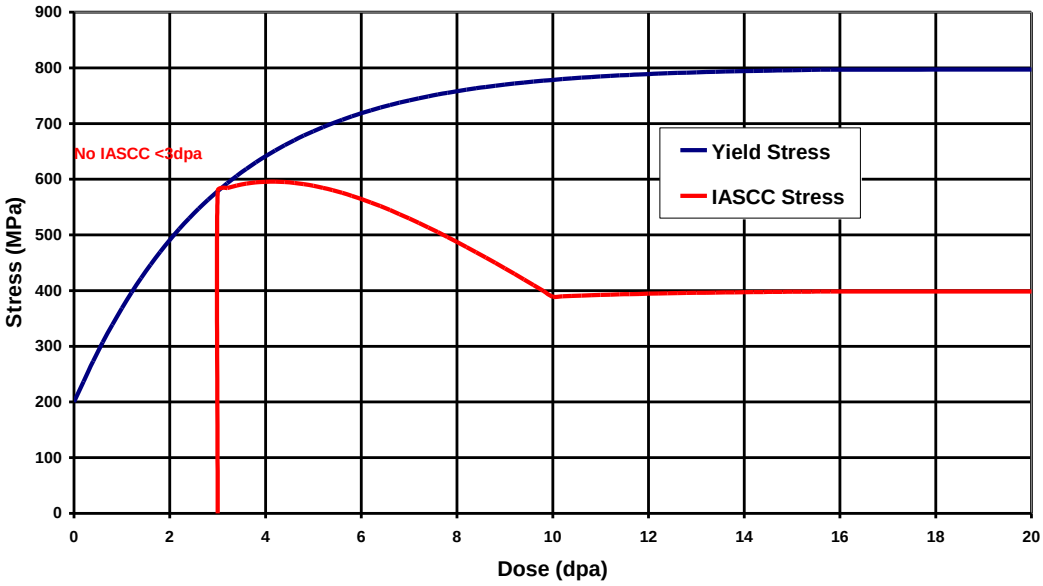

Figure 3-35
IASCC susceptibility stress for 304 SA at 330°C as a function of dose

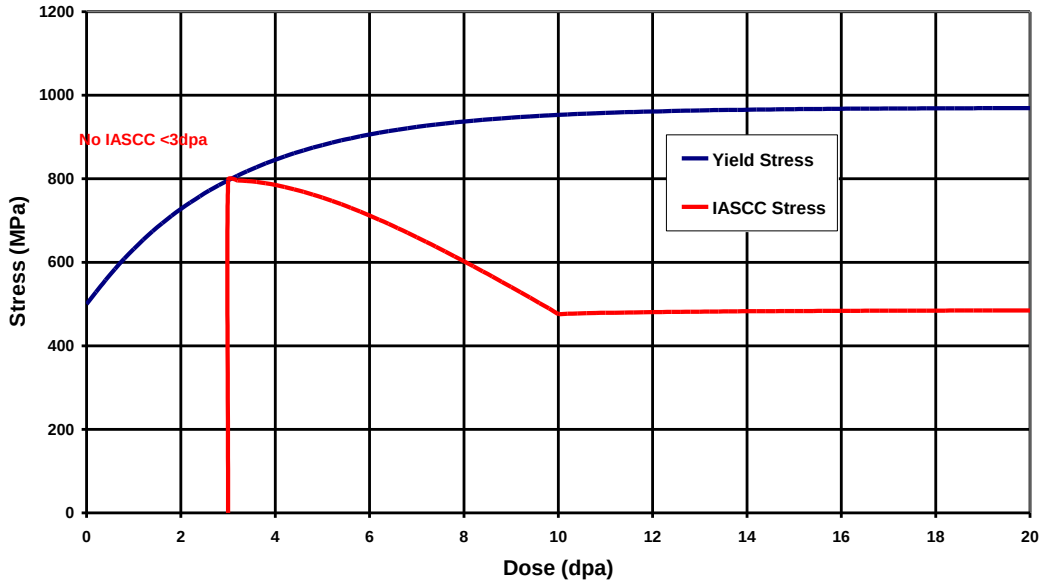

Figure 3-36
IASCC susceptibility stress for 316 CW at 330°C as a function of dose

Figures 3-35 and 3-36 do not account for the stress history; that is, a stress falling on the curves in these figures should be interpreted as the stress at which the component (such as a bolt) becomes susceptible to IASCC, and if the stress is maintained, failure is assumed to occur within a relatively short time (hundreds of hours). The failure model for IASCC monitors the stress at a material point and calculates a damage index as the ratio of the current stress to the IASCC threshold stress, which is the stress that falls on the susceptibility curves in Figures 3-35 and 3-36. Thus, the "damage index" can be viewed as the relative proximity, in stress space, to IASCC susceptibility. The damage index can change non-monotonically and continuously in time if the stress so varies. During shutdown periods, the IASCC susceptibility index can drop to zero. It is noted that merely exceeding unity in the damage index should not be interpreted as component failure. However, a damage-index value greater than unity with a relatively constant or monotonically increasing trend with time over a period of several hundred hours can be regarded as an indication of potential failure by IASCC.

3.9.3 Effects of Irradiation on Ductility

As previously covered, irradiation damage causes the material to harden and suffer a reduction in ductility. These effects appear in the stress-strain curve as higher yield and ultimate strengths, lower uniform and total elongations, and reduced strain hardening, as exhibited in Figures 3-26 through 3-29. Failure of the component purely due to the effects of irradiation on the material's mechanical properties is highly unlikely under normal service conditions. Nevertheless, a damage index is calculated for this potential condition, which is simply the larger of the two ratios—the effective strain to the total elongation (elastic + plastic), or the effective stress to the ultimate tensile strength.

3.9.4 Embrittlement Due to Void Swelling

The third form of damage formulated in the model is due to excessive void swelling, which can be caused by irradiation under unusually low dose rate at relatively high temperature [30, 35]. Under such conditions, there is evidence to indicate that stainless steel can become very brittle if the volumetric void swelling reaches 10% or greater [30, 35]. Brittle failure occurs at room temperature because the tearing modulus approaches zero when the void swelling reaches 10% [30, 35]. For purposes of engineering evaluations, it is recommended that a void swelling level of 5% be regarded as a warning condition for susceptibility to embrittlement. The damage index calculated in the model is simply the ratio of volumetric strain due to void swelling to the limiting void swelling value of 10%. It should be stated, however, that the damage index calculated in this manner does not account for the experimental conditions under which swelling-induced embrittlement was observed [30, 35], which, as previously noted, might be outside the PWR environment. Therefore, for such a damage index to be valid, the user must verify that the dose rate and temperature in the analysis are in the same range as the experimental data in References [30] and [35].

4
REFERENCES

4.1 Works Cited

1. H. Tang and J. Gilreath, "Aging Research and Management of PWR Vessel Internals." Presented at the 5th International Symposium on Contribution of Material Investigation to the Resolution of Problems Encountered in Pressurized Water Reactors, Royal Abbey of Fontevraund, Loire Valley, France, September 23–27, 2002.
2. *Materials Reliability Program: Determination of Operating Parameters of Extracted Bolts (MRP-52)*. EPRI, Palo Alto, CA: 2001. 1003076.
3. *Materials Reliability Program: Hot Cell Testing of Baffle/Former Bolts Removed from Two Lead PWR Plants (MRP-51)*. EPRI, Palo Alto, CA: 2001. 1003069.
4. *Materials Reliability Program: PWR Internals Age-Related Material Properties, Degradation Mechanisms, Models, and Basis Data—State of Knowledge (MRP-211, Revision 1)*. EPRI, Palo Alto, CA: 2017. 3002010270.
5. *Irradiated Austenitic Stainless-Steel Constitutive Model (IRADSS) Version 1.0*. EPRI, Palo Alto, CA: 2010. 1020215.
6. "Assessment and Management of Aging of Major Nuclear Power Plant Components Important to Safety: PWR Vessel Internals." IAEA-TECDOC-1110. International Atomic Energy Agency, October 1999.
7. C. Oland and D. Naus, "Degradation Assessment Methodology for Application to Steel Containments and Liners of Reinforced Concrete Structures in Nuclear Power Plant." ORNL/NRC/LTR-95/29. Oak Ridge National Laboratory, Oak Ridge, TN: 1995.
8. *Standard Handbook for Mechanical Engineers*, 7th Edition, McGraw-Hill Book Company, 1967.
9. *Reactor Handbook*, 2nd Edition, Volume I, "Materials." Interscience Publishers, Inc., New York, 1960, pp. 565–577.
10. K. Farrell, T. Byun, and N. Hashimoto, "Mapping Flow Localization Processes in Deformation of Irradiated Reactor Structural Alloys." ORNL/TM-2002/66. Oak Ridge National Laboratory, Oak Ridge, TN: 2002.
11. C. Albertini, A. Del Grande, and M. Montagnani, "Effects of Irradiation on the Mechanical Properties of Austenitic Stainless Steels Under Dynamic Loading." *Effects of Radiation on Structural Materials*, ASTM STP 683, J.A. Sprague and D. Kramer, Eds., American Society for Testing and Materials, 1979, pp. 546–556.
12. *ITER Material Properties Handbook*, ITER Document No. S 74 RE 1, 1997. Available from http://www-ferp.ucsd.edu/LIB/PROPS/ITER/

13. 2001 ASME Boiler & Pressure Vessel Code, Section II, Part D, Table TE-1, p. 651.

14. *Joint Owner's Baffle Bolt Program.* JOBB-CD Version 02.12. EPRI, Palo Alto, CA: 2002.

15. "Mechanical Properties Test Data for Structural Materials Quarterly Progress Report for Period Ending January 31, 1977." ORNL-5255. Oak Ridge National Laboratory, Oak Ridge, TN. pp. 69–70.

16. J. Robertson, I. Ioka, A. Rowcliffe, M. Grossbeck, and S. Jitsukawa, "Temperature Dependence of the Deformation Behavior of Type 316 Stainless Steel after Low Temperature Neutron Irradiation," *Effects of Radiation on Materials: 18th International Symposium*, ASTM STP 1325, R. Nanstad, M. Hamilton, F. Garner, and A. Kumar, Eds., American Society of Testing and Materials, Philadelphia, PA: 1997.

17. M. Horsten and M. de Vries, "Tensile Properties of Type 316L(N) Stainless Steel Irradiated to 10 Displacements per Atom," *Journal of Nuclear Materials 215-212*, Elsevier Science B.V., North Holland, 1994, pp. 514–518.

18. J. Nagakawa, "Calculation of radiation-induced stress relaxation," *Journal of Nuclear Materials 212-215*, Elsevier Science Publishers B.V., North-Holland, 1994.

19. M. Grossbeck, "Empirical relations for tensile properties of austenitic stainless steels irradiated in mixed-spectrum reactors," *Journal of Nuclear Materials 179-181*, Elsevier Science Publishers B.V., North-Holland, 1991.

20. H. McCoy, "Heat-to-Heat Variation Studies of Type 316 Stainless Steel," *Fuels and Materials Development Program Quarterly Progress Report for Period Ending March 31, 1974.* ORNL-TM-4620. Oak Ridge National Laboratory, Oak Ridge, TN. pp. 110–126.

21. C. Jaske, H. Mindlin, and J. Perrin, "Development of Elevated Temperature Fatigue Design Information for Type 316 Stainless Steel," *Instn Mech Engrs*, Conference Publication 13, 1973.

22. J-P. Massoud and P. Dubuisson, "Synthesis of the Irradiations in the Reactor BOR-60 and of the Post-Irradiation Tests." Joint Owner's Baffle Bolt Program, HT-27/02/009/A, JOBB-CD Version 02.12. EPRI, Palo Alto, CA: 2002.

23. J-P. Massoud and P. Dubuisson, "Samara Experiment: Results of the Tensile Tests." Joint Owner's Baffle Bolt Program, HT-41/01/005/A, JOBB-CD Version 02.12. EPRI, Palo Alto CA: 2001.

24. J-P. Massoud and P. Dubuisson, "Boris 4 Experiment: Description of the Experiment and Materials. Results of Mechanical Tests." Joint Owner's Baffle Bolt Program, HT-41/01/006/A, JOBB-CD Version 02.12, EPRI, Palo Alto, CA: 2001.

25. J-P. Massoud and P. Dubuisson, "Boris 3 Experiment: Description of the Experiment and Materials. Results of Mechanical Tests." Joint Owner's Baffle Bolt Program, HT-41/00/004/A, JOBB-CD Version 02.12. EPRI, Palo Alto, CA: 2000.

26. J-P. Massoud and P. Dubuisson, "Boris 2 Experiment: Description of the Experiment and Results of Tensile Tests." Joint Owner's Baffle Bolt Program, HT-41/99/015/A, JOBB-CD Version 02.12. EPRI, Palo Alto, CA: 1999.

27. AK Steel 304/304L Stainless Steel, Product Data Bulletin, 304/304L-B-11-01-99.

28. AK Steel 316/316L Stainless Steel, Product Data Bulletin, 316/316L-B-11-01-99.

29. M. Toloczko and F. Garner, "Stress and Temperature Dependence of Irradiation Creep of Selected FCC and BCC Steels at Low Swelling." *The Effects of Radiation on Materials: 21st International Symposium,* ASTM STP 1447, M. Grossbeck, T. Allen, R. Lott, and A. Kumar, Eds., ASTM International, West Conshohocken, PA, 2003.

30. *Materials Reliability Program: A Review of Radiation Embrittlement of Stainless Steels for PWRs (MRP-79).* EPRI, Palo Alto, CA: 2002. 1003524.

31. *Material Reliability Program Technical Basis Document Concerning Irradiation-Induced Stress Relaxation and Void Swelling in Pressurized Water Reactor Vessel Internals Components (MRP-50).* EPRI, Palo Alto, CA: 2001. 1000970.

32. H. Xu and S. Fyfitch, "Irradiation Creep and Stress Relaxation in PWRs: A Review of the Literature." Presented at the Tenth International Conference on Environmental Degradation of Materials in Nuclear Power Systems—Water Reactors, 2001.

33. K. Ehrlich, "Irradiation Creep and Interrelation with Swelling in Austenitic Stainless Steels," *Journal of Nuclear Materials 100,* North-Holland Publishing Company, 1981.

34. J. Bates and E. Gilbert, "Experimental Evidence for Stress Enhanced Swelling," *Journal of Nuclear Materials 59,* North-Holland Publishing Company, 1976.

35. F. Garner, "Irradiation Performance of Cladding and Structural Steels in Liquid Metal Reactors." Chapter 6, Vol. 10A, *Materials Science and Technology: A Comprehensive Treatment,* VCH Publishers (1994), pp. 419–543.

36. *In-Situ NDT Measurements of Irradiation-Induced Swelling in PWR Core Internal Components—Phase II: Testing of Irradiated Materials (MRP-178).* EPRI, Palo Alto, CA: 2004. 1009762.

37. *Material Reliability Program: Irradiated Austenitic Stainless-Steel Constitutive Model (IRADSS) Version 1—Installation and User's Manual for Version 3.12 of Constitutive Model for Irradiated Austenitic Stainless Steels for Use with ANSYS.* EPRI, Palo Alto, CA: 2010. 1020215.

38. J. Foster and J. Flinn, "Residual stress behavior in fast neutron irradiated SA AISI 304L stainless steel cylindrical tubing," J. Nucl. Mater. Vol. 89 (1980), p. 99.

39. A. Kozlov, E. Shcherbakov, S. Averin, and F. Garner, "The Effect of Void Swelling on Electrical Resistance and Elastic Moduli in Austenitic Steels," *Effects of Radiation on Materials: 21st International Symposium*. ASTM STP 1447, M. Grossbeck, Ed. ASTM International, West Conshohocken, PA, 2003.

40. *Materials Reliability Program: Cluster Dynamics Prediction of Void Swelling in Austenitic Stainless Steels Under PWR Conditions (MRP-321).* EPRI, Palo Alto, CA: 2011. 1022867.

4.2 Bibliography

D. Porter, G. Hudman, and F. Garner, "Irradiation creep and swelling of annealed Type 304L stainless steel at ~390°C and high neutron fluence," J. Nucl. Mater. Vol. 179–181 (1991), p. 581.

J. Garnier,"Thèse de Doctorat de l'Institut National Polytechnique de Grenoble" ("Doctoral Thesis of the National Polytechnic Institute of Grenoble"), 2007.

R. Stoller, "Modeling Dislocation Evolution in Irradiated Alloys," Metall. Trans. A, Vol. 21A (1990), p. 1829.

L. Mansur, "Irradiation creep by climb-enabled glide of dislocation resulting from preferred absorption of point defects," *Phil. Mag*. Vol. 39 (1979), p. 497.

P. Heald and M. Speight, "Point defect behaviour in irradiated materials," *Acta Metall.* Vol. 23 (1975), p. 1389.

J. Flinn and T. Kenfield, "Neutron swelling observations on austenitic stainless steels irradiated in EBR-II," *Proceedings of the Workshop on Correlation of Neutron and Charged Particle Damage*, Oak Ridge National Laboratory. Oak Ridge, TN: 1976. p. 253.

F. Garner and D. Porter, "Irradiation creep and swelling of AISI 316 to exposures of 130 dpa at 385-400°C," *J. Nucl. Mater*. Vol. 155–157 (1988), p. 1006.

Material Reliability Program: Development of Material Constitutive Model for Irradiated Austenitic Stainless Steels (MRP-135-Rev. 1). EPRI, Palo Alto, CA: 2010. 1020958.

A
TRANSLATED TABLE OF CONTENTS

DISCLAIMER OF WARRANTIES AND LIMITATION OF LIABILITIES

材料可靠性計畫: 輻照沃斯田鐵不銹鋼 (MRP-135, 第二次修訂) 材料組成模型的發展

3002013216

最後報導，2019年9月

EPRI專案經理
K. Amberge

EPRI 核子質量保證方案的所有或部分要件適用於本產品。

YES (NO)

美國電力研究院
地址：3420 Hillview Avenue, Palo Alto, California 94304-1338 ▪ PO Box 10412, Palo Alto, California 94303-0813 ▪ USA
+1 800.313.3774 ▪ +1 650.855.2121 ▪ askepri@epri.com ▪ www.epri.com

產品說明

壓水式反應器(PWR)的內部組件會受到與老化相關退化機制機制的影響，這可能需要在授權許可證延展過程中進行評估。為了評估與老化有關的退化機制對零件功能性的影響，空洞腫脹、蠕滑、應力鬆弛、延展性退化及破裂的綜合影響－所有的這些都是零件的幾何、輻照、溫度和負載的功能－均需要進行塑造和分析。本報告描述了316和 304型輻照不銹鋼的材料性能模型，該模型用於對受核電廠營運條件影響的PWR內部組件中的螺栓和焊接連接進行 工程評估。本報告是EPRI MRP-135，2010年3月第一次修訂版的更新。

背景

目前的壓水式反應器發電廠即將結束各自的授權許可期，許多核電廠已進入延長運營期。美國核能發電工業已經制定了管理反應器容器內部零件老化衰退的檢查評估指南。本報告中描述的模型將用於有限元素基本分析方法中。該模型考慮了溫度、冷加工和輻照對材料性能特性的影響，這些特性包括彈塑性應力-應變曲線、輻照增強的蠕變（或簡稱輻射蠕變）、空洞腫脹以及與主要損害機制有關的材料失效限制，例如輻照促進應力腐蝕開裂(IASCC)和輻照引起的脆化。如本版MRP-135所述，用於MRP-135第一次修訂版中組成模型的資料包含在新修訂的MRP-211報告中。

目標

- 提供適用於反應器內部零件使用條件的可用材料特性。
- 利用這些材料的特性，在長期反應器運營時，為壓水式反應器內部零組件的 工程評估目的，建造用於有限元素基本分析方法中的輻照材料－特定性能模型。

方法

主要研究人員根據現有文獻編製了一份不銹鋼材料特性的目錄，將這些特性記錄於MRP-211中，並將其納入反應壓水式反應器運營環境的不銹鋼材料性能的組成模型中。主要研究人員使用的其他訊息來源包括來自核電工業和 EPRI MRP 的實驗資料，包括反應器內部零件問題任務組和聯合所有人的擋板螺栓程序。本報告中描述的相關性和方程式代表了現有測試數據集的最佳配合趨勢，但是並非界限，並且尚未完成不確定性的統計評估。所以，這些相關性和方程式不適用於工程設計計算。該模型是為了在新資料可使用時進行接納，並被構造為可在二維和三維幾何圖形中應用的通用有限元素代碼中使用。

結果

本報告中分析描述了已開發的材料性能模型，並在用戶材料子程序中進行編程，使得採用商業上可以通用的有限元素電腦程式能夠適用於反應器內部零件的工程評定與評估成為可能。透過這種方式，各種設計的壓水式反應器內部零件進行了相同的分析處理，從而為分析者之間的 工程評估 提供了技術一致性。

申請、價值和使用

本報告中提出的材料模型的開發及其在零件工程評估方法中的實施核電工業反應器內部零件老化管理計畫的基本要素。

關鍵字
工程評估
有限元素分析
功能性
輻照性不銹鋼
材料組成模型
壓水式反應器(PWR)內部零件

目錄

插圖列表

表格列表

Programme de fiabilité des matériaux : élaboration d'un modèle constitutif de matériau pour les aciers inoxydables austénitiques irradiés (MRP-135, révision 2)

3002013216

Rapport final, septembre 2019

Chef de projet EPRI
K. Amberge

La totalité ou une partie des exigences du programme d'assurance qualité nucléaire EPRI (EPRI Nuclear Quality Assurance Program) s'appliquent à ce produit.

YES  NO

ELECTRIC POWER RESEARCH INSTITUTE
3420 Hillview Avenue, Palo Alto, California 94304-1338 ▪ PO Box 10412, Palo Alto, California 94303-0813 ▪ États-Unis
(+1) 800.313.3774 ▪ (+1) 650.855.2121 ▪ askepri@epri.com ▪ www.epri.com

DESCRIPTION DU PRODUIT

Les composants internes des réacteurs à eau pressurisée (PWR) sont soumis aux effets des mécanismes de dégradation liés au vieillissement, qui doivent être évalués dans le cadre du processus de renouvellement de concession. Pour évaluer les effets des mécanismes de dégradation liés au vieillissement sur la fonctionnalité des composants, il convient de modéliser et d'analyser les effets intégrés du gonflement des cavités, du fluage, de la détente des contraintes, de la dégradation de la ductilité et de la fissuration, qui sont tous fonction de la géométrie des composants, de l'irradiation, de la température et de la charge. Le présent rapport décrit un modèle de comportement de matériau pour l'acier inoxydable irradié de type 316 et de type 304 utilisé dans le cadre des évaluations d'ingénierie et des évaluations des raccords boulonnés et soudés dans les composants internes des PWR soumis aux conditions opérationnelles des centrales. Le présent rapport met à jour le document MRP-135, révision 1, de l'Electric Power Research Institute (EPRI), daté de mars 2010.

Contexte
Les périodes de concession de la génération actuelle de centrales PWR touchent à leur fin et plusieurs centrales ont déjà dû prolonger leur période d'exploitation. Aux États-Unis, le secteur de l'énergie nucléaire a élaboré des lignes directrices d'inspection et d'évaluation pour gérer la dégradation due au vieillissement dans les composants internes des cuves de réacteurs. Le modèle décrit dans le présent rapport doit être utilisé dans le cadre d'une méthodologie d'analyse par éléments finis. Le modèle prend en considération les effets de la température, du travail à froid et de l'irradiation sur les caractéristiques de comportement du matériau, dont notamment la courbe contrainte-déformation élasto-plastique, le fluage stimulé par l'irradiation (ou tout simplement fluage d'irradiation), le gonflement des cavités et les limites de défaillance de tout matériau liées aux mécanismes d'endommagement primaires, tels que la fissuration par corrosion sous contrainte induite par l'irradiation et la fragilisation induite par l'irradiation. Les données utilisées pour réviser les modèles de constitution dans le document MRP-135, révision 1, telles que décrites dans la présente révision du document MRP-135, figurent dans le rapport MRP-211 venant d'être révisé.

Objectifs
- Mettre à disposition des propriétés de matériau applicables aux conditions de service des composants internes des réacteurs.
- Élaborer, à l'aide de ces propriétés de matériau, un modèle de comportement constitutif pour les matériaux irradiés à utiliser dans le cadre d'une méthodologie d'analyse par éléments finis pour l'évaluation d'ingénierie et l'évaluation des composants internes des PWR pour un fonctionnement de réacteur à long terme.

Approche
Les enquêteurs principaux ont compilé une liste des propriétés matérielles de l'acier inoxydable à partir des publications disponibles, ont documenté ces propriétés dans MRP-211, puis les ont intégrées à la modélisation constitutive du comportement de l'acier inoxydable dans l'environnement opérationnel des PWR. Les enquêteurs principaux se sont également appuyés sur d'autres sources d'informations, dont des données expérimentales de l'industrie et des

programmes MRP de l'EPRI, tels que le groupe de travail sur les problèmes internes des réacteurs et le groupe conjoint de propriétaires pour les boulons de type baffle. Les corrélations et les équations fournies dans le présent rapport représentent les tendances relevées dans les jeux de données des essais existants, mais ne sont fournies qu'à titre indicatif, car aucune évaluation statistique d'incertitude n'a été réalisée. Par conséquent, ces corrélations et équations ne sont pas censées servir dans les calculs de conception d'ingénierie. Le modèle a été élaboré pour pouvoir accepter de nouvelles données lorsqu'elles seront disponibles et pour servir dans un code par éléments finis à usage général. Il peut être utilisé dans des applications géométriques à deux et trois dimensions.

Résultats
Le modèle de comportement de matériau élaboré, décrit analytiquement dans le présent rapport, est programmé dans une sous-routine utilisateur-matériau permettant d'adapter un programme informatique par éléments finis à usage général disponible sur le marché aux évaluations d'ingénierie et aux évaluations des composants internes des réacteurs. Ainsi, les composants internes des PWR de différents types font l'objet du même traitement analytique, assurant par là l'uniformité technique des évaluations d'ingénierie et autres évaluations parmi les analystes.

Applications, valeur et utilisation
L'élaboration du modèle de matériau faisant l'objet du présent rapport et sa mise en œuvre dans une méthodologie d'évaluation d'ingénierie de composants sont des éléments essentiels du programme de gestion du vieillissement des composants internes de réacteur du secteur.

Mots-clés
Évaluation d'ingénierie
Analyse par éléments finis
Fonctionnalité
Aciers inoxydables irradiés
Modèle constitutif de matériau
Composants internes de réacteur à eau pressurisée (PWR)

TABLE DES MATIERES

LISTE DES FIGURES

LISTE DES TABLEAUX

材料信頼性プログラム：照射されたオーステナイト系ステンレス鋼の材料構成モデルの開発（MRP-135、改訂 2 版）

3002013216

最終報告書　2019 年 9 月

EPRI プロジェクトマネージャー
K. Amberge

本成果物には、EPRI 原子力品質保証プログラム (Nuclear Quality Assurance Program) の要件の全てまたは一部が適用される。

YES (NO)

米国電力研究所
3420 Hillview Avenue, Palo Alto, California 94304-1338・PO Box 10412, Palo Alto, California 94303-0813・USA
+1.800.313.3774・+1.650.855.2121・askepri@epri.com・www.epri.com

成果物記述書

加圧水型原子炉　(PWR)内部構成機器は、経年に関連する劣化メカニズムの影響を受けるため、許認可更新プロセスの一部として評価しなければならない可能性が考えられる。構成機器の機能性に対する経年関連劣化メカニズムの影響を評価するには、ボイドスエリング、クリープ、応力緩和、延性の低下、ひび割れなど、構成機器の形状、照射、温度、負荷などによって変わるものの総合的な影響をモデル化して分析する必要がある。この報告書は、発電所の運転条件にさらされる PWR 内部構成機器のボルト締め部および溶接接続部の工学的評価およびアセスメントの実施で使用する照射ステンレス鋼タイプ 316 およびタイプ 304 の材料挙動モデルについて説明する。本報告書は、米国電力研究所 (EPRI) のMRP-135、改訂 1 版、2010 年 3 月の更新版である。

背景

現世代の PWR 発電所は、それぞれの許認可期間の終わりに近づいており、複数の発電所がすでに延長運転期間に入っている。米国の原子力業界は、原子炉圧力容器内部構造物の経年劣化を管理するための検査と評価のガイドラインを策定した。本レポートで説明されているモデルは、有限要素ベースの分析方法で使用される。このモデルでは、材料の挙動特性に対する温度、冷間加工、および照射の影響を考慮しているが、これには、弾塑性応力 / ひずみ曲線、照射強化クリープ (または単に照射クリープ)、ボイドスエリング、および照射誘起応力腐食割れや照射誘起脆化といった一次損傷メカニズムに関連する材料の破損限界が含まれる。MRP-135　　の現在の改訂で説明されているように、MRP-135 改訂 1 版の構成モデルを修正するために使用されるデータは、新たに改訂された MRP-211 レポートに含まれている。

目的

- 原子炉内部構成機器の使用条件に適用可能な材料特性を利用可能とすること
- それらの材料特性を使用して、長期原子炉運転下で PWR の内部構成機器の工学的評価とアセスメントのために有限要素ベースの分析方法で使用する照射された材料固有の構成的挙動モデルを構築すること

アプローチ

主任研究員は、入手可能な文献からステンレス鋼材料特性のリストをまとめ、これらの特性を MRP-211 で文書化し、PWR 運転環境を反映するステンレス鋼材料挙動の構成モデリングにこれらの特性を組み込んだ。主任研究員が使用するその他の情報源には、原子炉内部構造物問題タスクグループ (Reactor Internals Issues Task Group) や共同所有者のバッフルボルトプログラムなど、業界および EPRI MRP からの実験データが含まれる。本レポートに記載されている相関関係と式は、既存の試験データセットに対する最適な傾向を表しているが、これらは有界ではなく、不確実性の統計的評価は実行されていない。したがって、これらの相関と式は、工学設計の計算で使用することを意図したものではない。このモデルは、新しいデータが使用可能になったときにこれを受け入れるよ

う定式化されており、2 次元および 3 次元双方のジオメトリに適用される汎用有限要素コードで使用するように構築される。

結果

開発された材料挙動モデルは、本レポートで分析的に説明しているが、市販の汎用有限要素コンピュータプログラムを原子炉内部構造物の工学的評価とアセスメントの適用に適応させることを可能とするユーザ材料サブルーチンにプログラムされている。このように、様々な設計の　PWRの内部構成機器に対して同じ分析処理が施されるため、アナリスト間の工学的評価とアセスメントに技術的な均一性をもたらす。

適用、価値、および使用

本レポートで提示する材料モデルの開発と構成機器の工学的評価およびアセスメント方法の実装は、業界の原子炉内部構造物の経年管理プログラムの重要な要素である。

キーワード

工学的評価およびアセスメント
有限要素解析
機能性
照射ステンレス鋼
材料構成モデル
加圧水型原子炉 (PWR) 内部構成機器

目次

図一覧

表一覧

재료 신뢰성 프로그램: 조사한 오스테나이트 스테인리스강을 위한 재료 구성 모델의 개발(MRP-135, 개정 2)

3002013216

최종 보고서, 2019년 9월

EPRI 프로젝트 매니저
K. Amberge

미국 전력연구소(EPRI: ELECTRIC POWER RESEARCH INSTITUTE)
3420 Hillview Avenue, Palo Alto, California 94304-1338 ▪ PO Box 10412, Palo Alto, California 94303-0813 ▪ USA
+1.800.313.3774 ▪ +1.650.855.2121 ▪ askepri@epri.com ▪ www.epri.com

제품 명세

가압경수로(PWR) 내부구조물 기기는 운전 기간에 따른 성능 저하 메커니즘의 영향을 받기 마련이며, 이는 허가 갱신 과정의 일부로 평가되어야 할 수도 있습니다. 운전 기간에 따른 성능 저하 메커니즘이 기기의 기능성에 미치는 효과를 평가하기 위해서는 기포 팽창, 크리프, 응력 완화, 연성 성능 저하 및 균열(이들 모두 기기의 기하학적 조건, 방사선조사, 온도 및 하중의 함수)의 통합 효과를 모델로 만들어 분석할 필요가 있습니다. 본 보고서에서는 발전소 운전 조건에 영향 받는 가압경수로 내부구조물 기기에서 볼트 및 용접 연결 부위에 대한 엔지니어링 평가 및 사정을 수행하는 데 활용할 수 있도록 조사한 스테인리스강 316 및 304의 재료 행동 모델에 대해 기술하고 있습니다. 본 보고서는 EPRI의 2010년 3월의 MRP-135, 개정본 1의 최신본입니다.

배경

– 현재 가압경수로 발전소의 발전은 각 발전소의 운전 허가 기간이 종료될 시점에 다가가고 있으며, 많은 발전소가 이미 연장 운전 기간에 돌입했습니다. 미국의 원자력 산업계는 원자로 내부구조물의 운전 기간에 따른 성능 저하 문제를 관리하기 위한 검사 및 평가 지침을 개발했습니다. 본 보고서에 기술된 모델은 유한 요소 기반 분석 방법론에서 활용될 예정입니다. 이 모델은 온도, 냉간가공, 방사선조사 등이 재료 행동 특성에 미치는 효과를 고려하며, 그러한 재료 행동 특성에는 탄소성 응력-변형 커브, 조사 강화 크리프(또는 줄여서 조사 크리프), 기포 팽창, 그리고 조사 유기 응력 부식 균열 및 조사 유도 취화와 같은 주요 손상 메커니즘과 관련이 있는 재료의 고장 한계도 포함됩니다. MRP-135의 현 개정본에서 기술된 바대로, MRP-135, 개정본 1의 구성 모델을 개정하기 위해 이용한 데이터는 새롭게 개정된 MRP-211 보고서에 수록되어 있습니다.

목표

- 원자로 내부구조물 기기의 운전 조건에 적용할 수 있는 재료 속성을 활용할 수 있도록 하기 위함.
- 그와 같은 재료 속성을 활용함으로써 장기적인 원자로 운전 조건에서 가압경수로의 내부구조물 기기에 대해 엔지니어링 평가 및 사정을 수행하기 위한 유한 요소 기반 분석 방법론에서 사용할 조사한 재료 고유의 구성 행동 모델을 구성하기 위함.

접근책

– 주요 조사자들은 활용 가능한 문헌에서 스테인리스강 재료 속성 목록을 취합하고, 그러한 속성을 MRP-211에 문서화하며, 또한 그것들을 가압경수로 운전 환경에 반영하는 스테인리스강 재료 행동의 구성 모델링에 통합시켰습니다. 주요 조사자들이 활용한 추가 정보원에는 원자로 내부구조물 문제 과제단(Reactor Internals Issues Task Group) 및 합동 발주자 배블 볼트 프로그램(Joint Owner's Baffle Bolt Program)을 비롯하여 산업계와 EPRI MRP로부터의 실험 데이터가 포함되어 있습니다. 본 보고서에 기술된 상관관계와 방정식은 기존의 테스트 데이터 세트에 가장 적합한 트렌드를 대표적으로 보여주고 있지만, 한편으로는 이것들은 구속력이 없으며, 또한 불확실성에 대한 통계적 평가도

수행되지 않았습니다. 결과적으로, 이들 상관관계와 방정식은 엔지니어링 설계 계산에 사용할 의도는 없었습니다. 이 모델은 새로운 데이터가 활용 가능해지는 대로 새로운 데이터를 수용할 수 있도록 공식화시켰고, 또한 2차원 및 3차원 기하학에 모두 적용되는, 범용의 유한-요소 규격에서 사용할 수 있도록 구성되었습니다.

결과

– 본 보고서에서 분석적으로 기술한, 개발된 재료 행동 모델은 시중에서 구할 수 있는 범용 유한 요소 컴퓨터 프로그램을 원자로 내부구조물의 엔지니어링 평가 및 사정에 적응시킬 수 있도록 하는 사용자 재료 서브루틴(하부 경로)에 프로그래밍됩니다. 이와 같은 방식으로, 다양한 설계의 가압경수로 내부구조물 기기는 동일한 분석을 거침으로써 분석자들 사이에서 엔지니어링 평가 및 사정에 기술적 통일성을 기할 수 있도록 제공되고 있습니다.

적용, 가치, 이용

– 본 보고서에서 제시된 재료 모델과 그것을 기기 엔지니어링 평가 및 사정에서 구현시키는 일은 산업계의 원자로 내부구조물 노후화 관리 프로그램의 필수 요소입니다.

키워드

– 엔지니어링 평가 및 사정
유한-요소 분석
기능성
조사한 스테인리스강
재료 구성 모델
가압경수로(PWR) 내부구조물 기기

목차

그림 목록

도표 목록

The Electric Power Research Institute, Inc. (EPRI, www.epri.com) conducts research and development relating to the generation, delivery and use of electricity for the benefit of the public. An independent, nonprofit organization, EPRI brings together its scientists and engineers as well as experts from academia and industry to help address challenges in electricity, including reliability, efficiency, affordability, health, safety and the environment. EPRI also provides technology, policy and economic analyses to drive long-range research and development planning, and supports research in emerging technologies. EPRI members represent 90% of the electricity generated and delivered in the United States with international participation extending to 40 countries. EPRI's principal offices and laboratories are located in Palo Alto, Calif.; Charlotte, N.C.; Knoxville, Tenn.; Dallas, Texas; Lenox, Mass.; and Washington, D.C.

Together...Shaping the Future of Electricity

Program:

Pressurized Water Reactor Materials Reliability

3002013216

Electric Power Research Institute
3420 Hillview Avenue, Palo Alto, California 94304-1338 • PO Box 10412, Palo Alto, California 94303-0813 USA
800.313.3774 • 650.855.2121 • askepri@epri.com • www.epri.com